

ALGEBRAS WITH MATCHINGS AND LINK FLOER HOMOLOGY

PETER OZSVÁTH AND ZOLTÁN SZABÓ

ABSTRACT. We explain how to use bordered algebras to compute a version of link Floer homology. As a corollary, we also give a fast computation of the Thurston polytope for links in S^3 .

1. INTRODUCTION

The aim of this paper is to generalize the bordered construction of knot invariants from [9] to handle the case of links, giving a practical computation of a variant of link Floer homology for links in S^3 [14], which is sufficient to determine the Thurston polytope of such links. (The reader should compare with the computation of link homology using grid diagrams from [5]; see also [6, 8].)

As background, let \vec{L} be an oriented link with ℓ components. Such a link has a multi-variable Alexander polynomial $\Delta_L \in \mathbb{Z}[t_1^{\pm 1/2}, \dots, t_\ell^{\pm 1/2}]$. The oriented meridians for the link give an identification of $\mathbb{Z}[t_1^{\pm 1}, \dots, t_\ell^{\pm 1}]$ with the group-ring $\mathbb{Z}[H^1(S^3 \setminus L)]$; and in this way, we can view the Alexander polynomial Δ_L as defining for an (unoriented) link an element of $\mathbb{Z}[H^1(S^3 \setminus L)]$. As explained in [1], this polynomial can be written as a state sum of Kauffman states for a decorated link projection, with local contributions as shown in Figure 1.

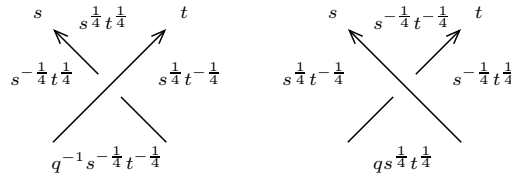


FIGURE 1. **Kauffman states for links.** Monomial contributions at each crossing of a Kauffman state. Monomials are in the variable q , whose exponent records the Maslov grading, and variables corresponding to the oriented strands, whose exponents record the Alexander gradings. The strand exiting on the top left resp. top right corresponds to the variable s resp. t .

Remark 1.1. *Note that there are two conventions in link (and knot) Floer homology, corresponding how the orientation of a link is encoded in a pointed Heegaard*

PSO was supported by NSF grant number DMS-1405114 and DMS-1708284.
 ZSz was supported by NSF grant numbers DMS-1606571 and DMS-1904628.

diagram. Since link Floer homology is invariant under reversing the orientation of all components, both conventions ultimately lead to the same invariant. Figure 1 is consistent with the orientation convention from [8]; it is opposite to the one from [10, Figure 1], which in turn follow the conventions from [11].

In [14], we defined a version of “link Floer homology”, $\widehat{HFL}(L)$, which is a finite-dimensional vector space over $\mathbb{F} = \mathbb{Z}/2\mathbb{Z}$. That group is equipped with two gradings, one with values in \mathbb{Z} , and another with values in an affine space $\mathbb{H} \subset \frac{1}{2}H_1(S^3 \setminus L; \mathbb{Z})$ for $H^1(S^3 \setminus L; \mathbb{Z})$. The subset $\mathbb{H} \subset \frac{1}{2}H_1(S^3 \setminus L; \mathbb{Z})$ consists of elements $\sum_{i=1}^{\ell} a_i \cdot [\mu_i]$ with

$$2a_i + \ell k(L_i, L \setminus L_i) \in 2\mathbb{Z},$$

for $i = 1, \dots, \ell$; where L_i denotes the i^{th} component of L . We denote the direct sum decomposition of link Floer homology

$$\widehat{HFK}(L) \cong \bigoplus_{d \in \mathbb{Z}, h \in \mathbb{H}} \widehat{HFK}_d(L, h).$$

Link Floer homology with $\ell > 1$ has two key features. One is its relationship with the Alexander polynomial:

$$\bigoplus_{d \in \mathbb{Z}, h \in \mathbb{H}} (-1)^d \dim(\widehat{HFL}_d(L, h))[h] = \left(\prod_{i=1}^{\ell} (\mu_i^{1/2} - \mu_i^{-1/2}) \right) \cdot \Delta_L,$$

where μ_i denotes the oriented meridian of the link component L_i . (See [14, Equation (1)].) Another is its relationship with the Thurston polytope. This is stated in terms of the *link Floer homology polytope* in $H^1(S^3 \setminus L; \mathbb{R})$, which is the convex hull of all $h \in \mathbb{H}$ with $\widehat{HFL}(L, h) \neq 0$. The Minkowski sum of the dual Thurston polytope with the symmetric hypercube in $H^1(S^3 \setminus L)$ with edge-length two is twice the link Floer homology polytope. (See [15, Theorem 1.1]; see also [7].)

We will consider diagrams \mathcal{D} for the projection of an oriented link \vec{L} . These diagrams are drawn on the xy plane, and we assume that they are generic in the following sense:

- the restriction of y is a Morse function, with at most one critical point for each y value
- the y -values of all crossings are distinct from each other and from the y -values of each critical point.

A *marked link diagram* \mathcal{D} is a projection of an oriented link \vec{L} together with a collection of basepoints, called *markers*, one on each component of L , and one of these markers is distinguished. (The distinguished marker is indicated by a star, and the others are indicated by a dot.) A marked link projection has two distinguished regions, which are the regions adjacent to the distinguished basepoint.

We call a marked link projection *canonically marked* if the marking on each component of the link is the global minimum of the height function restricted to that component; and the distinguished marker is at the global minimum of the height function on the entire projection. A *marked upper link diagram* is the restriction of a marked link projection to an upper halfplane. The upper link diagram is called *canonically marked* if only the closed components of the tangle have markings on

them, and those markings occur at the global minima of the height function restricted to the closed components. If we slice a canonically marked link diagram along a generic horizontal slice, the diagram falls into a canonically marked upper diagram (and a lower diagram). See Figure 2 for some examples.

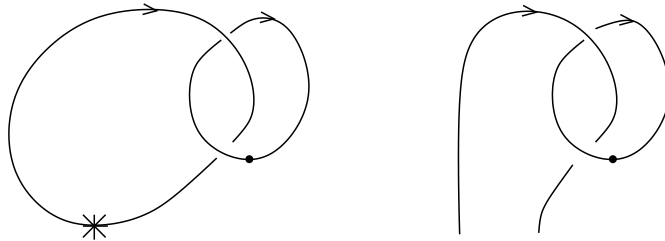


FIGURE 2. **Marked link projection.** At the left, a canonically marked link projection for the Hopf link. At the right, a canonically marked upper link diagram.

In the present paper, we define a type D structure $\widehat{R}(\mathcal{D})$ to each canonically marked upper link diagram. For a link in bridge position, where each marker is adjacent to the one of the two distinguished regions, the generators have an interpretation in terms of Kauffman states; see Section 3.6.

We also give a method for computing $\widehat{R}(\mathcal{D})$. Specifically, decompose \mathcal{D} into elementary pieces, cutting along horizontal slices, so that each piece consists of either a maximum, a crossing between adjacent strands, or a minimum, which can be marked or not. After introducing extra crossings if necessary, we can assume all the marked minima occur at the left of the diagram (i.e. they occur between the first two strands). To each elementary piece, we associate a type DA bimodule, so that the $\widehat{R}(\mathcal{D})$ is obtained as an iterated tensor product of the pieces. Indeed, to the pieces containing crossings, maxima, and unmarked minima the DA bimodules were already described in [9, Section].

Thus, the technical core of this paper is to compute the DA bimodule of a marked minimum (connecting the first two strands). With this computation, a suitable adaptation of the pairing theorem ([9, Theorem 9.1]; see also [4, Theorem 1.3]) completes the computation of $\widehat{R}(\mathcal{D})$.

Finally, the relationship with link Floer homology is given as follows. Suppose that \mathcal{D} is a canonically marked link diagram. Cutting it above the global minimum, we obtain a type D structure $\widehat{R}(\mathcal{D})$ over the algebra $\mathbb{F}[U_1, U_2]/U_1U_2 = 0$.

Theorem 1.2. *Let \mathcal{D} be a canonically marked diagram representing \vec{L} , and \mathcal{D}^+ be the upper diagram immediately above the global minimum. $\widehat{HFL}(\vec{L})$ is the homology of the chain complex obtained from $\widehat{R}(\mathcal{D})$ by specializing to $U_1 = U_2 = 0$.*

There are other versions of link Floer homology. One other variant is a module over a polynomial algebra $\mathbb{F}[U]$, associated to an oriented link \vec{L} , whose $U = 0$ specialization gives $\widehat{HFL}(L)$. This variant, and indeed some further enhancements of it, can also be computed by our techniques. The key point here is to develop

versions of the bimodule associated to a marked minimum, with more algebraic structure.

This paper is organized as follows. In Section 3 we describe the Heegaard diagrams relevant to this paper. We start by recalling Heegaard diagrams for links, following [14]. We generalize these notions, defining Heegaard diagrams associated to marked upper diagrams. These are a slight generalization of the Heegaard diagrams considered in [9]: the novelty here is that now we allow for closed components, provided that they are marked. This section also contains the corresponding generalization for middle diagrams. Finally, we describe the Heegaard diagram associated to a marked link projection generalizing slightly the Heegaard diagram of a knot projection as defined in [11].

In Section 2, we recall various versions of link Floer homology which can be computed using our methods. (The most general version we compute here depends also on an additional choice of distinguished link component.)

In [9], upper Heegaard diagrams give rise to curved type D structures over an algebra \mathcal{C} , while the middle diagrams can be extended to bimodules over a larger algebra \mathcal{B} . We review notation in Section 4.

In Section 5, we explain how to generalize the holomorphic constructions from [9] to associate modules to marked Heegaard diagrams. In Section 5.3, we adapt the pairing theorem from [9] to the case of marked diagrams.

In Section 6, we algebraically define DA modules, which are associated to marked minima. In Section 7, we verify that the algebraic construction indeed agrees with the construction defined using holomorphic methods.

In Section 8, we assemble the pieces to compute link Floer homology. We obtain Theorem 1.2 as a corollary of an algebraically enhanced version, Theorem 8.3.

Acknowledgements. The authors wish to thank Nate Dowlin, Robert Lipshitz, and Andy Manion for helpful conversations.

2. LINK FLOER HOMOLOGY

Let L be an ℓ -component link. Choose an orientation on each component of L , and choose also a distinguished component. We denote this data \vec{L}^* . We find it convenient to label the components $\{L_i\}_{i=1}^\ell$ of L so that L_1 is the distinguished component.

Consider polynomial algebra whose generators are labelled $w_1, z_1, \dots, w_\ell, z_\ell$, where we think of w_i as corresponding to the link component L_i with its given orientation and z_i as corresponding to L_i with its opposite orientation.

Specializing the construction from [14] (which we recall in detail in Section 3 below), there is a version of link Floer homology, which is a chain complex over the ring

$$\mathcal{R} = \mathbb{F}[w_1, z_1, \dots, w_\ell, z_\ell]/w_1 z_1 = 0.$$

Specifically, let \mathcal{H} be a 2ℓ pointed Heegaard diagram representing \vec{L}^* , equipped with 2ℓ basepoints labelled $(w_1, z_1, \dots, w_\ell, z_\ell)$ (so that w_i, z_i represent L_i). We can form $CFL(\vec{L}^*)$ the free \mathcal{R} -module generated by Heegaard states, and with

differential determined by

$$\partial \mathbf{x} = \sum_{\mathbf{y} \in \mathbb{T}_\alpha \cap \mathbb{T}_\beta} \sum_{\{\phi \in W(\mathbf{x}, \mathbf{y})\}} \# \widehat{\mathcal{M}}(\phi) \left(\prod_{i=1}^{\ell} w_i^{n_{w_i}(\phi)} z_i^{n_{z_i}(\phi)} \right) \cdot \mathbf{y},$$

where $\widehat{\mathcal{M}}(\phi)$ is a moduli space of pseudo-holomorphic Whitney disks in the homotopy class specified by ϕ . Let $HFL(\vec{L}^*)$ denote the homology of this chain complex, viewed as a module over \mathcal{R} . We define relative gradings so that if $\phi \in \pi_2(\mathbf{x}, \mathbf{y})$, then

$$\begin{aligned} \mathbb{A}(\mathbf{x}) - \mathbb{A}(\mathbf{y}) &= (n_{z_1}(\phi) - n_{w_1}(\phi), \dots, n_{z_\ell}(\phi) - n_{w_\ell}(\phi)) \\ \mathbf{m}(\mathbf{x}) - \mathbf{m}(\mathbf{y}) &= \mu(\phi) - 2 \sum_{w_i} n_{w_i}(\phi). \end{aligned}$$

To give an absolute Maslov grading, we require that the specialization of the complex to $z_1 = \dots = z_\ell = 1$, which has homology isomorphic to $\mathbb{F}[U]$ (where each w_i acts as multiplication by U), should have its generator supported in Maslov grading equal to zero. Equivalently, if we set $w_1 = \dots = w_\ell = 0$ and $z_1 = \dots = z_\ell = 1$, and take the homology of the resulting complex, then we obtain a graded group which contains a non-zero, homogenous element of Maslov grading 0, and no homogeneous generators with positive Maslov grading.

An absolute Alexander grading can also be specified by a certain symmetry of grid homology; cf. Equation (2.1) below.

The link complex above can be thought of as giving a version of the knot Floer homology of the three-manifold obtained as large surgery on the distinguished component. Dependence of the construction on the distinguished component can be removed in various algebraic specializations. For instance, one could set $w_i z_i = 0$ for all $i = 1, \dots, \ell$ in CFL , and then take homology to obtain an invariant of the underlying oriented link \vec{L} . Or one could form the specialization with $z_1 = \dots = z_\ell = 0$. This invariant is referred to as *unblocked grid homology* (in the context of grid diagrams) in [8, Chapter 11]. Specializing further to $w_1 = \dots = w_\ell$ (i.e. with $z_1 = \dots = z_\ell = 0$) gives the *collapsed grid homology* in the terminology of [8, Chapter 8.2], which we denote here $HFL^-(\vec{L})$. Finally, setting all $w_i = 0 = z_i$ for all $i = 1, \dots, \ell$ gives the complex for computing $\widehat{HFL}(\vec{L})$ from the introduction (the *simply blocked grid homology*, in the terminology of [8]).

These specializations are perhaps more natural objects than $HFL(\vec{L}^*)$; and indeed we will typically consider the case of \widehat{HFL} and its bordered analogues as warm-ups; but we will also consider $HFL(\vec{L}^*)$, since it is the algebraically most general construction that we can compute using our present methods.

Finally, we recall the following useful a symmetry in link Floer homology. To this end, let \vec{L} be an oriented link, and \vec{L}' be the oriented link obtained by reversing the orientation of the i^{th} component of \vec{L} . We have the symmetry

$$(2.1) \quad \widehat{HFL}_d(\vec{L}, (s_1, \dots, s_\ell)) \cong \widehat{HFL}_{d-2s_i+\kappa_i}(\vec{L}', (s_1, \dots, s_{i-1}, -s_i, s_{i+1}, \dots, s_\ell))$$

where

$$\kappa_i = \ell k(L_i, L \setminus L_i) \in 2\mathbb{Z}.$$

(cf. [8, Proposition 11.4.2]). This identification removes the additive indeterminacy of the Alexander grading.

3. HEEGAARD DIAGRAMS AND MARKED LINK PROJECTIONS

In this section, we describe the Heegaard diagrams that will be used for marked links. In Section 3.1, we recall the Heegaard diagrams for oriented links from [14]. In Section 3.2, we generalize these to marked upper diagrams, which we further generalize in Section 3.3 to marked middle diagrams. In Section 3.4, we describe marked lower diagrams. In Section 3.6 we describe the Heegaard diagrams for marked link projections, generalizing the construction from [11].

3.1. Heegaard diagrams for links. Recall [14, Definition 3.7] that an oriented link \vec{L} can be represented by a Heegaard diagram,

$$(\Sigma_0, \boldsymbol{\alpha}, \boldsymbol{\beta}, w_1, z_1, \dots, w_\ell, z_\ell),$$

where:

(L-1) Σ_0 is a genus g surface with 2ℓ boundary components, labelled

$$w_1, z_1, \dots, w_\ell, z_\ell.$$

(L-2) $\boldsymbol{\alpha} = \{\alpha_1, \dots, \alpha_{g+\ell-1}\}$ is a set of pairwise disjoint, embedded curves.

(L-3) The surface obtained by cutting Σ_0 along the α -curves has ℓ components A_1, \dots, A_ℓ , each of which contains exactly one w -marked boundary component and one z -marked boundary component.

(L-4) $\boldsymbol{\beta} = \{\beta_1, \dots, \beta_{g+\ell-1}\}$ is another set of pairwise disjoint, embedded curves.

(L-5) The surface obtained by cutting Σ_0 along the β -curves consists of ℓ components B_1, \dots, B_ℓ , each of which contains exactly one w -marked boundary component and one z -marked boundary component.

(L-6) The two one-to-one correspondences between the w - and z -boundary components specified in Parts (L-3) and (L-5) coincide; i.e. if we can label all the boundary components and connected components so that A_i and B_i contain w_i and z_i .

The underlying three-manifold (which in our case will be S^3) is obtained by filling in the boundary components of Σ_0 with disks to obtain a Heegaard surface Σ , equipped with attaching circles $\boldsymbol{\alpha}$ and $\boldsymbol{\beta}$. This Heegaard diagram $(\Sigma, \boldsymbol{\alpha}, \boldsymbol{\beta})$ specifies the three-manifold. Thinking of the w and z -boundaries as inducing corresponding marked points in Σ , we can obtain a link by first connecting the w and z -markings by pairwise disjoint, embedded arcs in Σ that are disjoint from the $\boldsymbol{\alpha}$, and pushing it slightly into the α -handlebody; and then connecting the w and z -markings analogously in the β -handlebody. An orientation on this link is specified by demanding that the portion in the α -handlebody is oriented as arcs from w to z .

(Our w -markings $\{w_1, \dots, w_\ell\}$ resp. z -markings were denoted \mathbf{w} resp. \mathbf{z} in [14]; the w and z -markings correspond to the O -markings and X -markings respectively for grid diagrams [8]. The convention for the induced orientation on the link here is opposite to the one given in [14], but it is consistent with the one given for grid diagrams in [8].)

We will consider Heegaard diagrams satisfying the following property.

Definition 3.1. A periodic domain P is a two-chain in Σ_0 with

$$\partial P = \sum_i m_i [\alpha_i] + \sum_j n_j [\beta_j],$$

where $m_i, n_i \in \mathbb{Z}$. A periodic domain is called somewhere positive (resp. negative) if some local multiplicity is positive (resp. negative). The Heegaard diagram is called admissible if every non-zero periodic domain is somewhere positive (and hence also somewhere negative).

Note that we can think of these as two-chains in Σ with vanishing local multiplicity at the marked points corresponding to the various w_i and the z_i .

A Heegaard state for a $(\Sigma_0, \alpha, \beta, w_1, z_1, \dots, w_\ell, z_\ell)$ is a $g + \ell - 1$ -tuple of points $\{x_1, \dots, x_{g+\ell-1}\}$ with $x_i \in \alpha_{\sigma(i)} \cap \beta_i$, where σ is an element of the symmetric group on $g + \ell - 1$ letters.

3.2. Marked upper Heegaard diagrams. We modify the notion of upper Heegaard diagram from [9, Section 2] to include closed components.

Definition 3.2. A marked upper Heegaard diagram is the following data:

- a surface Σ_0 of genus g and $2n$ boundary components, labelled Z_1, \dots, Z_{2n} , and 2ℓ additional boundary components labelled $\widehat{w}_1, \widehat{z}_1, \dots, \widehat{w}_\ell, \widehat{z}_\ell$.
- a collection of disjoint, embedded arcs $\{\alpha_i\}_{i=1}^{2n-1}$, so that α_i connects Z_i to Z_{i+1} ,
- a collection of disjoint embedded closed curves $\{\alpha_i^c\}_{i=1}^{g+\widehat{\ell}}$ (which are also disjoint from $\alpha_1, \dots, \alpha_{2n-1}$),
- another collection of embedded, mutually disjoint closed curves $\{\beta_i\}_{i=1}^{g+n+\widehat{\ell}-1}$.

We require this data to also satisfy the following properties:

- (UD-1) For each $i \in \{1, \dots, 2n-1\}$, $j \in \{1, \dots, g+\widehat{\ell}\}$, and $k \in \{1, \dots, g+\widehat{\ell}+n-1\}$, α_i and α_j^c curves are transverse to β_k .
- (UD-2) Both sets of α - and the β -circles consist of homologically linearly independent curves (in $H_1(\Sigma_0)$).
- (UD-3) Each component $B_1, \dots, B_{n+\widehat{\ell}}$ of the surface obtained by cutting Σ_0 along $\beta_1, \dots, \beta_{g+\widehat{\ell}+n-1}$, is required to contain exactly two boundary components, which are either both of type Z , or one is of type z and the other is of type w .
- (UD-4) Each component $A_1, \dots, A_{\widehat{\ell}+1}$ of the the surface obtained by cutting Σ_0 along $\alpha_1^c, \dots, \alpha_{g+\widehat{\ell}}^c$, is required to either contain all the Z -components, or exactly one of the w -components and one of the z -components.
- (UD-5) Condition (UD-4) gives a one-to-one correspondence between the z -boundaries and the w -boundaries; Condition (UD-3) gives another one-to-one correspondence between the z -boundaries and the w -boundaries. We require that these two correspondences coincide.
- (UD-6) Together, the closed curves $\{\alpha_i^c\}_{i=1}^{g+\widehat{\ell}}$ and $\{\beta_i\}_{i=1}^{g+\widehat{\ell}+n-1}$ span a $2g + \widehat{\ell} + n - 1$ -dimensional subspace of $H_1(\Sigma_0; \mathbb{Z})$.

Remark 3.3. *An upper diagram specifies a three-manifold-with-boundary Y equipped with an $\widehat{\ell}$ -component, oriented link, and whose boundary is a sphere containing an embedded collection of $2n$ arcs. (Condition (UD-5) ensures that the oriented link indeed has $\widehat{\ell}$ components; Condition (UD-6) ensures that $H_1(Y; \mathbb{Z}) = 0 = H_2(Y; \mathbb{Z})$. Compare [13, Proposition 2.15].) When $g = 0$, the three-manifold Y is a three-ball.*

Condition (UD-4) gives a matching M on $\{1, \dots, 2n\}$ (a partition into two-element subsets), where $\{i, j\} \in M$ if Z_i and Z_j can be connected by a path that does not cross any β_k .

We will typically abbreviate the data

$$\mathcal{H}^\wedge = (\Sigma_0, \{Z_1, \dots, Z_{2n}\}, \{\widehat{w}_1, \dots, \widehat{w}_{\widehat{\ell}}\}, \{\widehat{z}_1, \dots, \widehat{z}_{\widehat{\ell}}\}, \\ \{\alpha_1, \dots, \alpha_{2n-1}\}, \{\alpha_1^c, \dots, \alpha_{g+\widehat{\ell}}^c\}, \{\beta_1, \dots, \beta_{g+\widehat{\ell}+n-1}\}),$$

and let $M(\mathcal{H}^\wedge)$ be the induced matching on $\{1, \dots, 2n\}$.

For upper diagrams, there are two natural generalizations of the notion of periodic domains and admissibility.

Definition 3.4. *A periodic domain is a two-chain in Σ_0*

$$\partial P = \sum_i m_i [\alpha_i^c] + \sum_j n_j [\beta_j],$$

with $m_i, n_i \in \mathbb{Z}$. A diagram is called admissible if every non-zero periodic domain has positive and negative local multiplicities.

Viewed as two-chains in Σ , rather than Σ_0 , the periodic domains we consider here have vanishing multiplicities at the punctures corresponding to \widehat{Z} , z , and w . In the terminology of [3], these are called *provincial periodic domains*.

To check admissibility, it helps to have the following observation. Number the connected components $\{A_1, \dots, A_{\widehat{\ell}}\}$ as in Condition (UD-4) so that A_i contains the markings w_i and z_i specifying L_i ; number the components $\{B_1, \dots, B_{\widehat{\ell}+n-1}\}$ so that their first $\widehat{\ell}$ components are also labelled so that B_i contains w_i and z_i . Then, it is easy to see that the periodic domains are spanned by the regions $A_i - B_i$.

When $\widehat{\ell} = 0$, the corresponding link is empty, and we are considering the upper diagrams from [9]. When $n = 0$, we are considering Heegaard diagrams for links as in Section 3.1. In particular, when $n = 0$ and $\ell = 1$, we can think of these as the double-pointed knot diagrams from [9].

Definition 3.5. *A Heegaard state for a marked upper diagram \mathcal{H}^\wedge is a $d = g + \widehat{\ell} + n - 1$ -tuple of points \mathbf{x} in the intersection of the various α - and β -curves, distributed so that each β -circle contains exactly one point in \mathbf{x} , each α -circle contains exactly one point in \mathbf{x} , and no more than one point lies on any given α -arc.*

For an upper Heegaard diagram with $2n$ outputs, and a Heegaard state \mathbf{x} , we let

$$\alpha(\mathbf{x}) = \{i \in \{1, \dots, 2n-1\} \mid \mathbf{x} \cap \alpha_i \neq \emptyset\}.$$

3.3. Marked middle diagrams. We will enlarge marked upper diagrams by gluing them to marked middle diagrams.

Definition 3.6. A marked middle diagram is the following data:

- a surface Σ_0 of genus g and $2m$ boundary components, which we think of as incoming boundary components, labelled $\check{Z}_1, \dots, \check{Z}_{2m}$, $2n$ boundary components, which we think of as outgoing boundary components, labelled $\hat{Z}_1, \dots, \hat{Z}_{2n}$ and $2\ell_{\parallel}$ additional boundary components labelled

$$w_{\parallel}^{\parallel}, z_{\parallel}^{\parallel}, \dots, w_{\ell_{\parallel}}^{\parallel}, z_{\ell_{\parallel}}^{\parallel}.$$

- a collection of disjoint, embedded arcs $\{\check{\alpha}_i\}_{i=1}^{2m-1}$, so that $\check{\alpha}_i$ connects \check{Z}_i to \check{Z}_{i+1} ,
- a collection of disjoint, embedded arcs $\{\hat{\alpha}_i\}_{i=1}^{2n-1}$ (which are also disjoint from the $\check{\alpha}_j$), so that $\hat{\alpha}_i$ connects \hat{Z}_i to \hat{Z}_{i+1}
- a collection of disjoint embedded closed curves $\{\alpha_i^c\}_{i=1}^{g+\ell_{\parallel}}$ (which are also disjoint from $\check{\alpha}_i$ and $\hat{\alpha}_j$)
- another collection of embedded, mutually disjoint closed curves $\{\beta_i\}_{i=1}^{g+m+n+\ell_{\parallel}-1}$.

We require this data to also satisfy the following properties:

- (MD-1) All the α -arcs and curves are transverse to the various β_k .
- (MD-2) Both sets of α - and the β -circles consist of homologically linearly independent curves (in $H_1(\Sigma_0)$).
- (MD-3) The span of the homology classes of the curves $\{\alpha_i^c\}_{i=1}^{g+\ell_{\parallel}}$ is linearly independent of the span of $\{\beta_i\}_{i=1}^{g+\ell_{\parallel}+m+n-1}$ in $H_1(\Sigma_0; \mathbb{Z})$.
- (MD-4) The surface obtained by cutting Σ_0 along $\beta_1, \dots, \beta_{g+\ell_{\parallel}+m+n-1}$, which has $m+n+\ell_{\parallel}$ connected components $B_1, \dots, B_{m+n+\ell_{\parallel}}$, is required to contain exactly two boundary components in each component, so that each w -boundary is paired with a z -boundary.
- (MD-5) Each component $A_1, \dots, A_{\ell_{\parallel}+1}$ of the surface obtained by cutting Σ_0 along $\alpha_1^c, \dots, \alpha_{g+\ell_{\parallel}}^c$ is required to contain either all the Z -components, or exactly one of the w -component and one z -component. We call the induced one-to-one correspondence between the w - and z -boundary components the α -matching.

Sometimes, we abbreviate the data of a middle diagram \mathcal{H}^{\parallel} . Moreover, we will write $\check{\partial}\mathcal{H}^{\parallel} = \check{Z}_1 \cup \dots \cup \check{Z}_{2m}$ $\hat{\partial}\mathcal{H}^{\parallel} = \hat{Z}_1 \cup \dots \cup \hat{Z}_{2n}$.

Definition 3.7. The $B_1, \dots, B_{m+n+\ell_{\parallel}}$ induce a matching M^{\parallel} on the boundary components

$$\{\check{Z}_1, \dots, \check{Z}_{2m}, \hat{Z}_1, \dots, \hat{Z}_{2n}, w_{\parallel}^{\parallel}, \dots, w_{\ell_{\parallel}}^{\parallel}, z_{\parallel}^{\parallel}, \dots, z_{\ell_{\parallel}}^{\parallel}\},$$

called the β -matching.

Definition 3.8. A periodic domain is a relative two-chain for (Σ_0, \check{Z}) with

$$\partial P = \sum_i m_i [\alpha_i^c] + \sum_j n_j [\beta_j],$$

with $m_i, n_i \in \mathbb{Z}$, satisfying for all $\{i, j\} \in \widetilde{M}$,

$$\mathfrak{w}_{\widetilde{Z}_i}(P) = \mathfrak{w}_{\widetilde{Z}_j}(P).$$

A diagram is called *admissible* if every non-zero periodic domain has both positive and negative local multiplicities.

Definition 3.9. A matching \widetilde{M} on $\{\widetilde{Z}_1, \dots, \widetilde{Z}_{2m}\}$ is said to be *compatible* with M^\parallel if the equivalence relation generated by \widetilde{M} and M^\parallel has the property that each equivalence class has either exactly one w -marking and exactly one z -marking, or it has exactly two \widehat{Z} -markings, and this induced matching of the w and z -markings coincides with the one-to-one α -matching, as defined in Condition (MD-5).

Geometrically, we can associate a one-manifold W^\parallel with decorations to a middle diagram. Start from the zero-manifold whose points correspond to the boundary components of Σ_0 . To each component B_j we associate an arc connecting the two boundary components. To each component A_i connecting w_i and z_i , we associate an arc connecting w_i to z_i , which we call a *marked arc*. To the incoming matching \widetilde{M} , we associate another one-manifold \widetilde{W} , consisting of arcs connecting the pairs of points in the matching. The compatibility condition can be phrased as follows: each closed component of the one-manifold $W^\parallel \cup \widetilde{W}$ contains exactly one marked arc.

We will need the following notion of a compatible orientation on $W^\parallel \cup \widetilde{W}$ to define the bimodule associated to a middle diagram and an incoming matching.

Definition 3.10. A one-manifold with markings is a one-manifold W , equipped with a set of embedded arcs, each of whose endpoints are labelled with an z and an w . A compatible orientation on the one-manifold with markings is an orientation of W whose restriction to each marked arc orients it as a path from the w -marking to the z -marking. We will use these compatible orientations to define the bimodule associated to a middle diagram.

The definition of Heegaard states (Definition 3.5) generalizes immediately to the case of middle diagrams, with the understanding that now the number of β -circles is given by $d = g + \ell_\parallel + m + n - 1$.

For a Heegaard state \mathbf{x} in a middle diagram, let

$$\begin{aligned} \check{\alpha}(\mathbf{x}) &= \{i \in \{1, \dots, 2m - 1\} \mid \check{\alpha}_i \cap \mathbf{x} \neq \emptyset\} \\ \widehat{\alpha}(\mathbf{x}) &= \{i \in \{1, \dots, 2n - 1\} \mid \widehat{\alpha}_i \cap \mathbf{x} \neq \emptyset\}. \end{aligned}$$

Definition 3.11. An extended marked middle diagram is a middle diagram, together with two new boundary components, Z_0^\parallel and Z_1^\parallel , four new α -arcs, $\check{\alpha}_0$, $\check{\alpha}_{2m}$, $\widehat{\alpha}_0$, and $\widehat{\alpha}_{2n}$, and two new β -circles β_0 and β'_0 , arranged so that

- $\check{\alpha}_0$ connects \widetilde{Z}_1 to Z_0^\parallel ,
- $\widehat{\alpha}_0$ connects \widehat{Z}_1 to Z_0^\parallel ,
- β_0 separates Z_0^\parallel from all the other boundary components of Σ_0 ,
- $\check{\alpha}_{2n}$ connects \widetilde{Z}_{2m} to Z_1^\parallel
- $\widehat{\alpha}_{2m}$ connects \widehat{Z}_{2n} to Z_1^\parallel
- β'_0 separates Z_1^\parallel from all the other boundary components of Σ_0 .

- if we fill in Z_0^\parallel and Z_1^\parallel with disks, and delete the newly introduced arcs and circles, the result is a middle diagram.

For an extended middle diagrams, $\check{\alpha}(\mathbf{x}) \subset \{0, \dots, 2m\}$ and $\hat{\alpha}(\mathbf{x}) \subset \{0, \dots, 2n\}$.

(Extended marked middle diagrams are the natural adaptation of the notion of extended middle diagrams as defined in [13].)

3.4. Marked lower diagrams.

Definition 3.12. A marked lower diagram is a marked middle diagram with no outgoing boundary components (or arcs), and one additional β circle, i.e. the β circles are numbered $\{\beta_i\}_{i=1}^{g+n+\check{\ell}}$, with $n > 0$, together with one distinguished w-z-pair, \check{w}_1, \check{z}_1 , so that Conditions (MD-4) and (MD-5) are replaced by the following:

(LD-5) The surface obtained by cutting Σ_0 along $\beta_1, \dots, \beta_{g+\check{\ell}+n}$, has $n+1$ components $B_1, \dots, B_{n+\check{\ell}+1}$, each of which contains exactly two boundary components, which can be of the following types:

- B_i contains w_j and z_j with $j \neq 1$
- B_i contains w_1 and a component of type Z
- B_i contains z_1 and a component of type Z
- B_i contains two boundary components of type Z .

(LD-6) Each component $A_1, \dots, A_{\check{\ell}}$ of the surface obtained by cutting Σ_0 along $\alpha_1^c, \dots, \alpha_{g+\check{\ell}}^c$ is required to contain either all the Z components and \check{w}_1 and \check{z}_1 ; or exactly one \check{w}_j and exactly one \check{z}_j (for $j \neq 1$).

For a lower diagram with boundary $\check{Z}_1, \dots, \check{Z}_{2m}, \check{w}_1, \check{z}_1, \dots, \check{w}_{\check{\ell}}, \check{z}_{\check{\ell}}$, we can define the associated matching M (exactly as in M^\parallel for middle diagrams). Similarly, given a matching \check{M} on $\{\check{Z}_1, \dots, \check{Z}_{2m}\}$, we can define a compatibility condition with M as in Definition 3.9. Letting W be the marked one-manifold associated to the lower diagram, we can form the marked one-manifold $W \cup \check{W}$. For lower diagrams, the orientation on $W \cup \check{W}$ is uniquely specified by the compatibility condition of Definition 3.10.

3.5. Gluing diagrams. If \mathcal{H}^\wedge is an upper diagram, and \mathcal{H}^\parallel is a middle diagram, and an identification $\partial\mathcal{H}^\wedge = \check{\partial}\mathcal{H}^\parallel$, we can form a new upper diagram $\mathcal{H}^\wedge \cup_{\check{Z}} \mathcal{H}^\parallel$. For example, if $\{\hat{w}_1, \dots, \hat{w}_{\hat{\ell}}\}$ and $\{w_1^\parallel, \dots, w_{\ell_\parallel}^\parallel\}$ resp. $\{\hat{z}_1, \dots, \hat{z}_{\hat{\ell}}\}$ and $\{z_1^\parallel, \dots, z_{\ell_\parallel}^\parallel\}$ denote the w-marked resp. z-marked boundaries of \mathcal{H}^\wedge and \mathcal{H}^\parallel , then the w- and z-marked boundaries of $\mathcal{H}^\wedge \cup_{\check{Z}} \mathcal{H}^\parallel$ are

$$\{\hat{w}_1, \dots, \hat{w}_{\hat{\ell}}, w_1^\parallel, \dots, w_{\ell_\parallel}^\parallel\} \quad \text{and} \quad \{\hat{z}_1, \dots, \hat{z}_{\hat{\ell}}, z_1^\parallel, \dots, z_{\ell_\parallel}^\parallel\}.$$

If \mathcal{H}^\wedge and \mathcal{H}^\parallel are admissible, then the glued diagram is admissible, as well.

3.6. Heegaard diagrams from link projections. A knot projection has a naturally associated doubly-pointed Heegaard diagram, as described in [12], studied further in [9]. We must modify this algorithm to take into account marked edges (which are treated slightly differently from the distinguished edge). The construction is summarized in Figure 3.

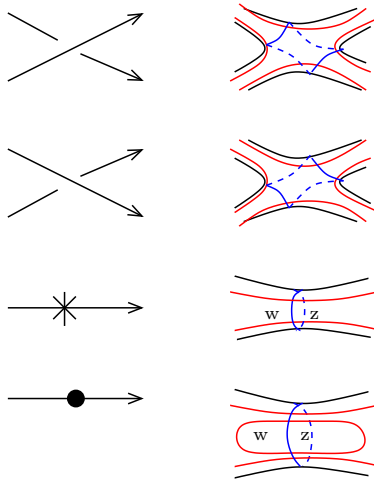


FIGURE 3. Heegaard diagram for a marked minimum.

The resulting diagram is called the *small Heegaard diagram associated to a marked link projection*.

Proposition 3.13. *There is a $2^{\ell-1}$ -to-one correspondence between Heegaard states in the above diagram with the Kauffman states of [1]. The Maslov and Alexander gradings are given by multiplying the monomial local contributions as in Figure 1.*

The above proposition follows quickly from the methods from [12]. We will see it as an easy consequence of Proposition 3.20 below.

There is a basis for the periodic domains for the link projection which correspond to the non-distinguished components of the link: their local multiplicity is 1 in the portion of the Heegaard diagram around the given link component. Thus, the diagram constructed above is not admissible. To construct an admissible diagram, we will need some additional data.

Definition 3.14. *A marked link diagram is called relevant if the following two properties hold:*

- *the marking on each component occurs at the minimum of the height function restricted to the link components*
- *the distinguished marking occurs at the global minimum of the height function.*
- *each minimum is leftmost; i.e. the intersection of the horizontal line through each minimum meets the rest of the link to the right of the minimum.*

The first two properties are the canonical marking of the diagram discussed in the introduction; the second property implies that the markings are adjacent to the infinite (marked) region.

Fix a relevant link diagram, connect the marking on some component to the adjacent strand by a dotted arc. We then isotope each such dotted arc which is otherwise disjoint from the knot projection. We shrink this dotted arc, to form an

admissibility marker. Crossings in the diagram and admissibility markers together can be thought of as *generalized crossings*. In particular, at each admissibility marker, there are also four adjacent regions, which we think of as N , S , W , and E . We mark these so that the S region is part of the infinite region, and the short dotted arc runs W to E , as shown in Figure 4.

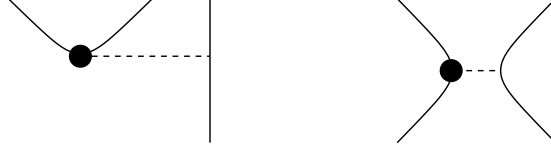


FIGURE 4. **Admissibility markers.** A portion of the canonically marked diagram on the left is decorated by a dotted arc as shown, and isotoped to the picture on the right.

The regions in the diagram will be thought of as the connected components of the complement of the diagram, together with the $\ell - 1$ dotted arcs at each marking. Two of these regions are distinguished by being adjacent to the distinguished edge.

We extend the notion of Kauffman states for relevant diagrams, as follows. Once again, a Kauffman state associates one of the four adjacent regions at each crossing. Moreover, our extended Kauffman states also can associate one of the two adjacent regions at each admissibility marker: these regions can be N or W (but not E or S). Our Kauffman state is constrained by the requirement that there is a one-to-one correspondence between generalized crossings and the indistinguished regions in the diagram.

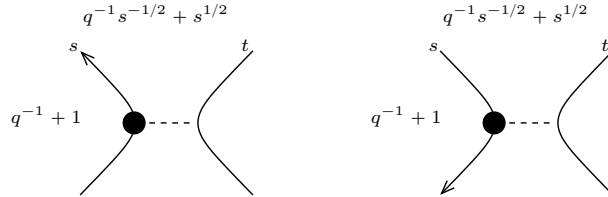


FIGURE 5. **Local Kauffman states at an admissibility arc.** There are two local Kauffman states (N and W) that can appear in a generalized Kauffman state near an admissibility marking. These contribute the displayed monomial in q and s .

To construct the *Heegaard diagram associated to the relevant link projection*, we associate the piece of diagram from Figure 6 to each admissibility marker (and the pieces associated to crossings and specially marked edge as in Figure 3).

For a relevant link diagram, we will identify the Kauffman states with the Heegaard states of the associated link diagram (c.f. Proposition 3.20 below), in a way that respects the the Maslov and Alexander gradings. Our verification use methods of Kauffman [1], suitably adapted.

Specifically, recall that two Kauffman states \mathbf{x} and \mathbf{y} are connected by a *clock move* if there are two crossings where \mathbf{x} and \mathbf{y} are different and the same everywhere else,

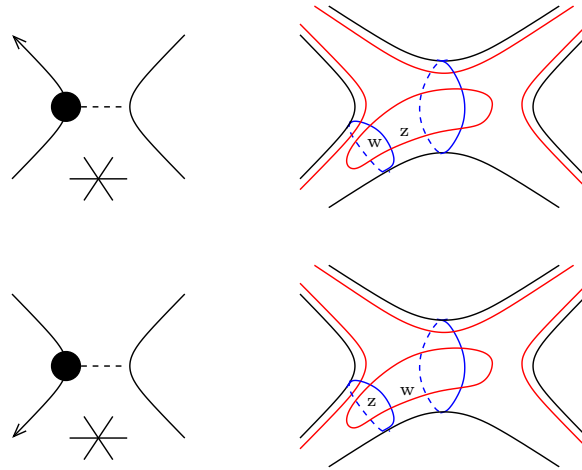


FIGURE 6. **Heegaard diagram for an admissibility arc.** The admissibility marker at the left is replaced by the piece of Heegaard diagram on the right. (The star is drawn to remind the reader that the Southern quadrant is adjacent to the distinguished edge.)

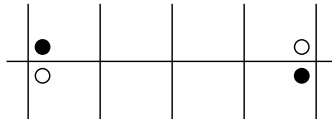


FIGURE 7. **Schematic of two Kauffman states (black and white) connected by a clock move.** The two Kauffman states are required to agree at all other crossings; the edges in the horizontal line are required not adjacent to either distinguished region.

and there is a path of edges connecting those two crossings which is never adjacent to one of the two distinguished regions, see for example Figure 7. According to Kauffman [1], any two Kauffman states for a connected projection can be connected by a sequence of clock transformations. We need the following variant of this fact:

Definition 3.15. *Let P be a knot diagram with a distinguished crossing x , whose four quadrants are labelled N, S, E, W . The NS resolution of P at x is the diagram obtained from P by resolving the crossing so that the N and S become connected to one another. The EW resolution is the other resolution.*

Definition 3.16. *Let C be a set of crossings of an oriented marked planar diagram, and mark the quadrants of the projection at each $c \in C$ as N, W, E, S . We say that a Kauffman state is of type C - NW , if at each $c \in C$, the Kauffman state is in the N quadrant or the W -quadrant.*

Definition 3.17. *A set S of Kauffman states is called clock connected if any two elements of S can be connected by a sequence of clock transformations, each of which connects two elements of S .*

In this language, Kauffman's clock theorem states that for a connected projection, the set of all Kauffman states is non-empty and clock-connected.

Proposition 3.18. *Fix an oriented planar diagram P . Let P be an oriented marked planar diagram, and choose a collection C of crossings in P , which are all adjacent to one region R , which is one of the two distinguished regions in P . Label the quadrants at each $c \in C$ so that the quadrant contained in R is labelled with an S . Suppose that the diagram P' obtained as the NS resolution of P at each $c \in C$ is connected. Then, the set of Kauffman states of type C - NW is clock-connected.*

Proof. We prove this by induction on the number of elements in C . If C is empty, then the theorem follows from Kauffman's Clock theorem applied to P .

The Kauffman states that are of type N at $c \in C$ correspond to Kauffman states in the NS resolution of P_c of P at c , and the clock transformations between such Kauffman states correspond to clock transformations in P_c . Thus, it follows by the inductive hypothesis, the set of Kauffman states of type C - NW for which at least one crossing in C is of type N is clock-connected.

Consider any Kauffman state of type C - W . Since the Kauffman states for P are clock-connected (Kauffman's theorem again), for any Kauffman state x_1 of type C - W , we can find a sequence x_1, \dots, x_m of Kauffman states so that x_i is connected to x_{i+1} by a clock move, and x_m is not of type C - W . Consider the smallest i for which x_i is not of type C - W . This means that there is one $c \in C$ so that x_i is not of type W at c , but x_{i-1} is of type W at c . Since the S quadrant is distinguished, it follows that x_i must be of type N at c . \square

For a relevant diagram, we consider Kauffman states, now connected generalized Kauffman states. In particular, at the admissibility markers, these states are required to occupy the N and the W quadrants only.

Corollary 3.19. *For a relevant link diagram which is connected in the complement of the edge markers, the set of generalized Kauffman states is clock-connected.*

Proof. This follows from Proposition 3.18 (thinking of the generalized Kauffman states as Kauffman states for a connected diagram, which are constrained to occupy positions N and W). \square

Proposition 3.20. *The Heegaard diagram associated to a relevant link diagram is an admissible Heegaard diagram, and its Heegaard states correspond to Kauffman states for the admissibly marked diagram. Moreover, the Alexander and Maslov gradings are as specified in Figures 1 and 5.*

Proof. For admissibility we argue as follows. There is an ordering on link components, L_1, \dots, L_ℓ , in increasing order of the value of the global minimum; for example, L_ℓ contains the special minimum. The space of periodic domains is spanned by domains P_i supported in a neighborhood of each L_i for $i = 2, \dots, \ell$. Find the largest k so that P_k appears in a given expansion. If it occurs with positive local multiplicity, then we can find a small bigon in the Heegaard diagram for the corresponding admissibility marker (i.e. the bigon from y to x locally in Figure 8) where the periodic domains has negative local multiplicity. This verifies admissibility.

Label the Heegaard states locally near each admissibility arc as in Figure 8.

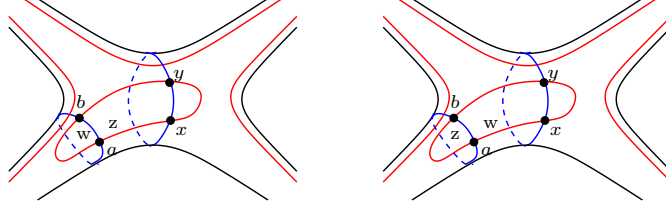


FIGURE 8. **Local Heegaard states near the admissibility markers.**

This gives a correspondence between Heegaard states and Kauffman states: a and b locally correspond to the two monomials in the northern quadrants of Figure 5; x and y locally correspond to the two terms in the western quadrant in Figure 5.

We check next that the local contributions of these Kauffman states agree with the Alexander and Maslov gradings, up to overall additive constants.

Suppose that the marked strand is oriented upwards; i.e. that we are considering the Heegaard diagram on the left in Figure 8. First we compare the contributions of states associated to the same quadrant, using domains that are locally contained in the marked region; i.e. by inspecting Figure 8. For example, there is a bigon in $\pi_2(a, b)$ (i.e. with Maslov grading 1) that crosses z but not w . It follows that for two states occupying the same corners,

$$\begin{aligned} \mathbb{A}(b) &= \mathbb{A}(a) + [\mu_s] & \mathbf{m}(b) &= \mathbf{m}(a) + 1 \\ \mathbb{A}(x) &= \mathbb{A}(y) & \mathbf{m}(y) &= \mathbf{m}(x) + 1, \end{aligned}$$

where here $[\mu_s] \in H_1(S^3 \setminus L)$ is the generator which is the meridian for the s^{th} component of L .

Next, as in the proof of [11, Theorem 1.2], we check that the Kauffman contributions transform as expected under clock moves. This is done in Figure 9.

A similar computation can be done when the strand is oriented oppositely, to complete the identification of the Maslov and Alexander gradings, up to an overall additive indeterminacy.

To remove the additive indeterminacy of the Maslov grading, we argue as in [11, Lemma 2.5]. After a sequence of handleslides back over z -marked regions, we obtain a new diagram, where the β -curve at a each crossing is replaced by meridian, which meets α -curves belonging to two (rather than possibly) four regions. Specifically, label the four edges at each crossing. The new β -curve, then, will be a meridian for the second edge we encounter as we traverse the knot. Once again, there is a correspondence between Heegaard states and Kauffman states for the resulting diagram, with the understanding that Kauffman states for the new diagram are allowed to be adjacent only to this second edge. In [11], we proved that there was one such state. (In that paper, we were considering the “penultimate”, which is the third edge we encounter, instead of the second; but this discrepancy is due to our different orientation conventions on the knot.) That generator in turn correspond to $2^{\ell-1}$ Heegaard states, according to whether we are using locally the intersection point a or b ; and all of these live on in homology. The absolute gradings are

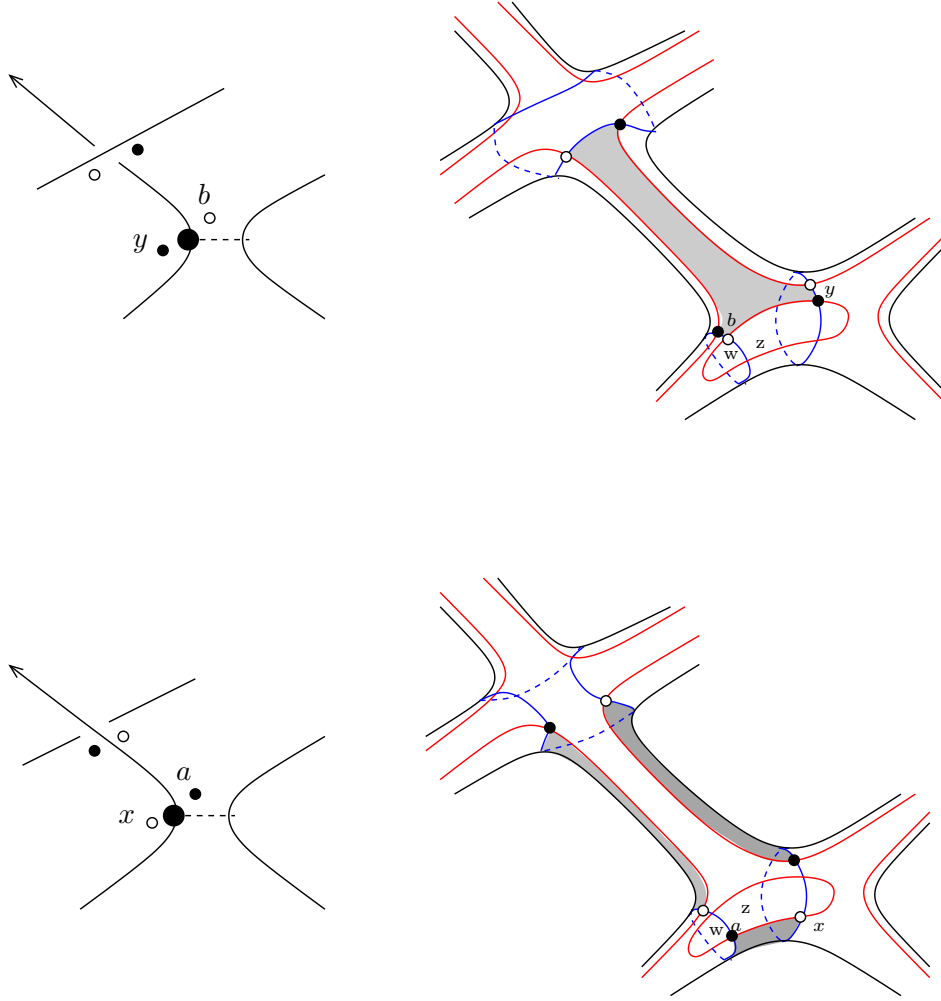


FIGURE 9. Checking local contributions.

verified by noting that maximal Maslov grading is 0. Since handleslides preserve the Maslov grading of the generator, the formula follows.

The symmetry from Equation (2.1) holds. This can be seen on the level of local Kauffman contributions (Figures 1 and 5). Specifically, if s is the variable associated to a given strand, then substituting $s \mapsto (q^2 s)^{-1}$ to the monomial contribution gives $q^{\pm 1/2}$ times the monomial contribution obtained by reversing the orientation of the strand, where \pm is simply the sign of the crossing. Thus, for a given Kauffman state \mathbf{x} , if

$$\mathbb{A}_{\bar{L}}(\mathbf{x}) = (s_1, \dots, s_\ell) \quad \text{and} \quad \mu_{\bar{L}}(\mathbf{x}) = d$$

then

$$\mathbb{A}_{\bar{L}'}(\mathbf{x}) = (s_1, \dots, s_{i-1}, -s_i, s_{i+1}, \dots, s_\ell) \quad \text{and} \quad \mu_{\bar{L}'}(\mathbf{x}) - 2s_i = \mu_{\bar{L}}(\mathbf{x}) - \kappa_i.$$

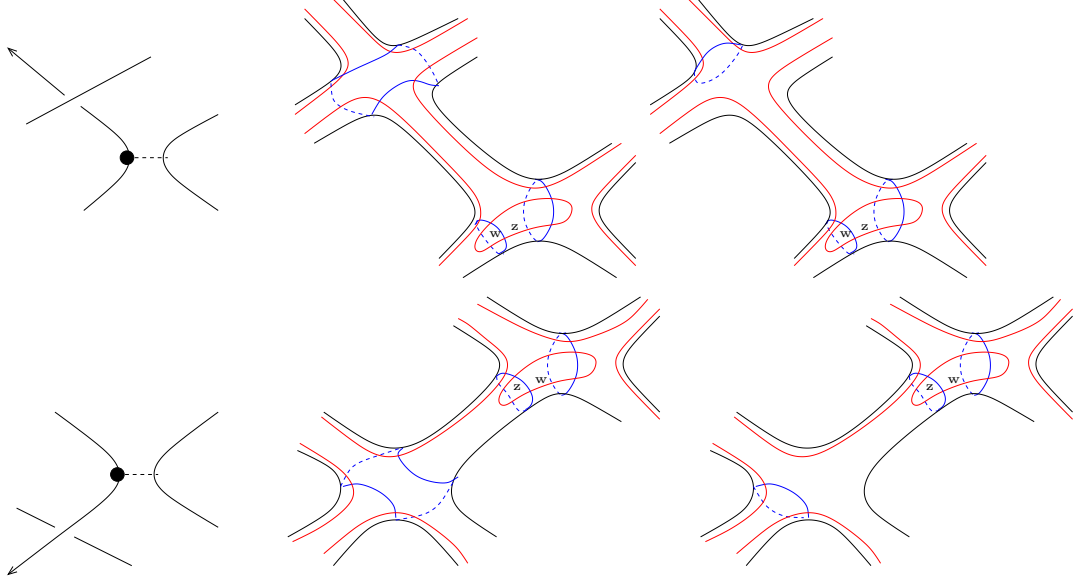


FIGURE 10. **Kauffman state with Maslov grading zero.** Handle-slide locally over the z marking to obtain the Heegaard diagram on the right.

Since the chain complexes $\widehat{CFL}(\vec{L})$ and $\widehat{CFL}(\vec{L}')$ are isomorphic, we have verified Equation (2.1). The absolute Alexander gradings follow. \square

These diagrams can be sliced: a generic horizontal slice in a marked link projection corresponds to a collection of curves in the Heegaard surface that decomposes the Heegaard surface into a marked upper diagram and a marked lower diagram.

4. ALGEBRA

4.1. The bordered algebras. Recall the bordered algebra $\mathcal{B}(m, k)$ constructed in [10, Section 3.2]. As in [9], we specialize to the case $\mathcal{B}(n) = \mathcal{B}(2n, n)$, equipped with its idempotent ring $I(n) = I(2n, n)$. We will consider various subrings of its idempotent ring $I(n)$, as follows:

Definition 4.1. Let $I_{*\geq i}$ denote the subalgebra of I generated by idempotent states $\mathbf{x} = x_1 < \dots < x_k$ with $x_1 \geq i$; similarly, let $I_{*\leq i}$ denote the subalgebra of I generated by \mathbf{x} so that $x_k \leq i$. Let $I_{i \leq * \leq j} = I_{*\geq i} \cdot I_{*\leq j}$.

The algebra $\mathcal{B}(n)$ has a subalgebra $I_{1 \leq * \leq 2n-1} \cdot \mathcal{B}(n) \cdot I_{1 \leq * \leq 2n-1}$, denoted $\mathcal{C}(n)$ in [9]. This is naturally the ring over which the type D structures of an upper diagram are defined. More precisely, upper diagrams come equipped with a matching M on $\{1, \dots, 2n\}$. The matching specifies a curvature

$$\mu_0^M = \sum_{\{i,j\} \in M} U_i U_j.$$

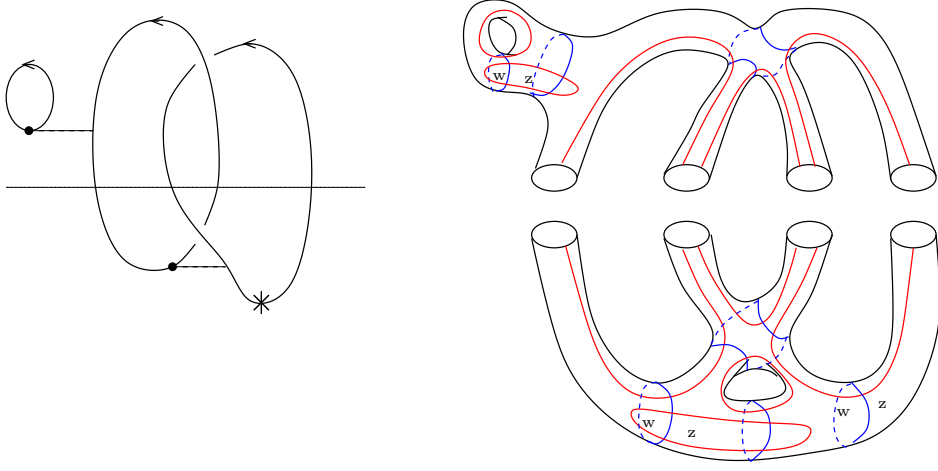


FIGURE 11. **Slicing the Heegaard diagram of a marked link projection.** Start from the marked link projection on the left, sliced in half along the dotted line, to obtain the upper and lower marked diagrams on the right.

Given an upper Heegaard diagram \mathcal{H}^\wedge with $2n$ Z -boundary components and ℓ w -boundaries (and ℓ z -boundaries), we can associate a matching M on $\{1, \dots, 2n\}$. Let \mathcal{C}^\star be the algebra $\mathcal{C}^\star(n) \otimes \mathbb{F}[w_1, z_1, \dots, w_\ell, z_\ell]$ equipped with curvature μ_0^M . We will show in Section 5 how to construct an associated curved type D structure $\mathcal{C}^\star R(\mathcal{H}^\wedge)$. (In the case where $\ell = 0$, this is the construction from [9].)

Recall that \mathcal{B} has a grading, called the Δ -grading, which is -1 times the sum of all the weights of the algebra elements; e.g. $\Delta(L_i) = -1/2$, $\Delta(U_i) = -1$.

4.2. **Simplifying type D structures.** Let

$$\mathfrak{B} = \mathcal{B}(n) \quad \text{or} \quad \mathcal{B}(n) \otimes \mathbb{F}[w_1, z_1, \dots, w_\ell, z_\ell]$$

for some value of n (and ℓ). The algebra \mathfrak{B} is filtered by weight, in the following sense. There is an ideal \mathfrak{B}_+ generated by algebra elements with positive weight (either in \mathcal{B} or in the w_i or z_i) with quotient $\mathfrak{B}/\mathfrak{B}_+ \cong I_n$.

Suppose that ${}^{\mathfrak{B}^\star}X$ is a (curved) type D structure.

Lemma 4.2. *A finitely generated type D structure ${}^{\mathfrak{B}^\star}X$ is homotopy equivalent to a different type D structure ${}^{\mathfrak{B}^\star}X'$ with the property that*

$$\delta^1: X' \rightarrow \mathfrak{B}_+ \otimes X'.$$

Proof. This is a familiar argument in homological algebra: if $\delta^1(X') \notin \mathfrak{B}_+ \otimes X'$, there are $p, q \in X'$ so that $\delta^1(p) \in q + \mathfrak{B}_+ \otimes X'$. Define a new homotopy equivalent type D structure with two fewer generators obtained by contracting the arrow from p to q . The result now follows by induction on the rank of X (as a left I -module). \square

4.3. **The algebra \mathcal{A}'' .** In [9], we introduced also algebras $\mathcal{A}''(n, M)$ where M is a matching on $\{1, \dots, 2n\}$. The algebra is obtained by adding adding elements $\{E_i\}_{i=1}^{2n}$ to $\mathcal{B}(2n, n+1)$. These elements satisfy the relations $E_i^2 = 0$,

$$[E_i, E_j] = \begin{cases} 1 & \text{if } \{i, j\} \in M \\ 0 & \text{otherwise} \end{cases}$$

The algebra is equipped with a differential satisfying $dE_i = U_i$.

In Section 12.3, we introduced a DD bimodule ${}^{\mathcal{B}^*, \mathcal{A}''} \mathcal{K}$, as follows. Fix $n \geq 1$ and a matching M on $\{1, \dots, 2n\}$, and let $\mathcal{A}'' = \mathcal{A}''(n, M)$, $\mathcal{B}^* = \mathcal{B}^*(n, M)$. Generators of ${}^{\mathcal{B}^*, \mathcal{A}''} \mathcal{K}$, as a vector space, correspond to n -element subsets $\mathbf{x} \subset \{0, \dots, 2n\}$, i.e. I -states for $\mathcal{B}(2n, n)$. Let $K_{\mathbf{x}}$ be the generator corresponding to \mathbf{x} . The left $I(2n, n) \otimes I(2n, n+1)$ -module structure is specified by

$$(\mathbf{I}_{\mathbf{x}} \otimes \mathbf{I}_{\{0, \dots, 2n\} \setminus \mathbf{x}}) \cdot K_{\mathbf{x}} = K_{\mathbf{x}}.$$

The differential is specified by the element

$$A = \sum_{i=1}^{2n} (L_i \otimes R_i + R_i \otimes L_i) + \sum_{i=1}^{2n} U_i \otimes E_i \in \mathcal{B} \otimes \mathcal{A}'',$$

$$\delta^1: \mathcal{K} \rightarrow \mathcal{B} \otimes \mathcal{A}'' \otimes \mathcal{K}.$$

by $\delta^1(v) = A \otimes v$.

4.4. **Working over \mathcal{C}^* .** In this paper, we will consider type D structures over \mathcal{B}^* which are actually induced by type D structures over \mathcal{C}^* . We write such type D structures ${}^{\mathcal{B}^*} \iota_{\mathcal{C}^*} \boxtimes^{\mathcal{C}^*} Y$. Concretely, a type D structure ${}^{\mathcal{B}^*} Y$ is of this type if $\mathbf{I}_{1 \leq * \leq 2n-1} \cdot Y = Y$.

The first simple observation we will use about such type D structures is the following:

Lemma 4.3. *If ${}^{\mathcal{B}^*} \iota_{\mathcal{C}^*} \boxtimes^{\mathcal{C}^*} Y \simeq {}^{\mathcal{B}^*} \iota_{\mathcal{C}^*} \boxtimes^{\mathcal{C}^*} Y'$, then ${}^{\mathcal{C}^*} Y \simeq {}^{\mathcal{C}^*} Y'$.*

Proof. Our morphisms (and homotopies) of type D structures are, by definition, left I -equivariant. The result follows easily. \square

Lemma 4.4. *If*

$${}^{\mathcal{B}^*} X' \simeq {}^{\mathcal{B}^*} \iota_{\mathcal{C}^*} \boxtimes^{\mathcal{C}^*} Y,$$

and $\delta^1: X' \rightarrow \mathcal{B}_+^* \otimes X'$, then in fact δ^1 takes X to $\mathcal{C}_+^* \otimes X'$.

Proof. Suppose that X' has some element p with the property that $\mathbf{I}_{\mathbf{x}} \cdot p = p$ with 0 or $2n \in \mathbf{x}$. Then, the homotopy equivalence implies that

$$p = \delta^1 \circ h + h \circ \delta^1;$$

and our hypothesis on δ^1 ensures that the right hand side is in $\mathcal{B}_+ \otimes X$. This contradicts the fact that $p \in I(n) \otimes X$. \square

In view of the above lemma, if X is any type D structure

$${}^{\mathcal{B}^*} X \simeq {}^{\mathcal{B}^*} \iota_{\mathcal{C}^*} \boxtimes^{\mathcal{C}^*} Y,$$

we can find an explicit form for ${}^{\mathcal{C}^*} Y$ by applying the algorithm of Lemma 4.2.

4.5. Boundedness and tensor products. Our type DA bimodules over $\mathcal{B}(n) \otimes \mathbb{F}[w_1, z_1, \dots, w_\ell, z_\ell]$ will typically be bounded above in Maslov grading; but not below. After all, each variable w_i and z_i drops Maslov grading by one.

Definition 4.5. Let ${}^{\mathcal{A}}X_{\mathcal{B}}$ be a DA bimodule over algebras \mathcal{A} and \mathcal{B} . A type DA bimodule is called unital if

$$\delta_{k+1}^1(\mathbf{x}, a_1, \dots, a_k) = \begin{cases} \mathbf{x} & \text{if } k = 1 \text{ and } a_1 = 1 \\ 0 & \text{if } k > 1 \text{ and some } a_i = 1. \end{cases}$$

A type DA bimodule is called bounded if for every integer M (which one can think of as a negative integer with large absolute value) there is an N so that $\Delta(\delta_{k+1}^1(\mathbf{x}, a_1, \dots, a_k)) \geq M$ we can conclude that $\sum_{i=1}^k \Delta(a_i) \geq N$.

Our type DA bimodules will be both bounded and unital.

Proposition 4.6. Let \mathfrak{B}_i^* be algebras of the form $\mathcal{B}(n)$ or $\mathcal{B}(n) \otimes \mathbb{F}[w_1, z_1, \dots, w_\ell, z_\ell]$ for $i = 1, 2$. If ${}^{\mathfrak{B}_2^*}X_{\mathfrak{B}_1^*}$ is a curved type DA bimodule which is strictly unital, bounded, and graded. Let \mathfrak{B}_1^*Y be a finitely generated type D structure which is graded. Then, the sums defining type D structure on $X \boxtimes Y$ are finite.

Proof. Gradings give a lower bound on $\delta(\mathbf{x} \otimes \mathbf{y})$, and hence, by the boundedness of X , a lower bound on the grading of $a_1 \otimes \dots \otimes a_k$. Unitality then gives the desired upper bound on k . \square

5. HOLOMORPHICALLY DEFINED MODULES

We sketch here the fairly straightforward modifications needed to adapt the modules from [9] to the case of links.

5.1. Modules for upper diagrams. Let \mathcal{H}^\wedge be an admissible marked upper diagram with $2n$ boundary circles $\hat{Z}_1, \dots, \hat{Z}_{2n}$. Let \widehat{M} be the induced matching. Our aim here is to define a curved type D structure over the algebra

$$\widehat{\mathcal{C}} = \mathcal{C}(n) \otimes \mathbb{F}[w_1, \dots, w_\ell, z_1, \dots, z_\ell],$$

where ℓ denotes the number of w -markings (and z -markings) in \mathcal{H}^\wedge , and the curvature is specified by the matching \widehat{M} .

Given an upper state \mathbf{x} , we define

$$\widehat{\mathbf{I}}(\mathbf{x}) = \{1, \dots, 2n - 1\} \setminus \alpha(\mathbf{x})$$

as in [9]; the following definition of $\widehat{b}(\phi)$ is also obtained from there:

Definition 5.1. Let $\phi \in \mathcal{D}(\mathbf{x}, \mathbf{y})$. Define $b_0(\phi)$ to be the homogenous element $b \in \mathcal{B}_0(n) \otimes \mathbb{F}[w_1, z_1, \dots, w_\ell, z_\ell]$ characterized by the following properties that

- $\widehat{\mathbf{I}}(\mathbf{x}) \cdot b \cdot \widehat{\mathbf{I}}(\mathbf{y}) = b$; and
- for all $i = 1, \dots, 2n$, $w_i(b)$ is the average of the local multiplicities of ϕ in the two elementary domains adjacent to Z_i .
- The w_i exponent of $b_0(\phi)$ is given by $n_{w_i}(\phi)$ and the z_i exponent of $b_0(\phi)$ is given by $n_{z_i}(\phi)$.

Let $\widehat{b}(\phi)$ denote the induced element in $\mathcal{B}(n) \otimes \mathbb{F}[w_1, z_1, \dots, w_\ell, z_\ell]$.

There is a Δ grading on the algebra, which is given by -1 times the total weight of an algebra element. In particular,

$$\Delta(w_i) = \Delta(z_i) = -1.$$

If W is an oriented one-manifold with boundary $\{1, \dots, 2n\}$ and $n + \ell$ components, we have an induced Alexander grading in the algebra characterized by

$$\begin{aligned} \mathfrak{A}(b \otimes \prod_{i=1}^{\ell} w_i^{a_i} z_i^{b_i}) &= \sum_{\{i,j\} \in M} (\omega_i(b) - \omega_j(b)) e_{\{i,j\}} \\ &\quad + \sum_{i=1}^{\ell} (b_i - a_i) e_i, \end{aligned}$$

where $e_{\{i,j\}}$ is the generator of $H^1(W; \mathbb{Z})$ corresponding to the component of W connecting i to j , and e_i is generator of $H^1(W; \mathbb{Z})$ corresponding to the i^{th} closed component of W .

Let $\mathbf{m}: \mathcal{D}(\mathbf{x}, \mathbf{y}) \rightarrow \frac{1}{2}\mathbb{Z}$ denote the Maslov index of the homotopy class of flows from \mathbf{x} to \mathbf{y} ; as in [2], this is computed by the formula

$$\mathbf{m}(B) = e(B) + n_{\mathbf{x}}(B) + n_{\mathbf{y}}(B),$$

where $e(B)$ is the Euler measure of B .

Proposition 5.2. *There is a function $\mathbf{m}: \mathfrak{S}(\mathcal{H}^\wedge) \rightarrow \mathbb{Z}$ uniquely characterized up to an overall constant by the property that*

$$(5.1) \quad \mathbf{m}(\mathbf{x}) - \mathbf{m}(\mathbf{y}) = \mathbf{m}(\phi) - \Delta(b_0(\phi)).$$

Similarly, given an orientation the one-manifold W there is a function $\mathfrak{A}: \mathfrak{S}(\mathcal{H}^\wedge) \rightarrow \frac{1}{2}\mathbb{Z}^{n+\ell}$ with components $\mathfrak{A}_{\{i,j\}}$ corresponding to $\{i, j\} \in M$ characterized by

$$(5.2) \quad \mathfrak{A}(\mathbf{x}) - \mathfrak{A}(\mathbf{y}) = \mathfrak{A}(b_0(\phi)).$$

Proof. This is a straightforward adaptation of [9, Proposition 4.5]. If $\phi, \phi' \in \mathcal{D}(\mathbf{x}, \mathbf{y})$, then

$$\phi - \phi' = \sum_{i=1}^{\hat{\ell}} m_i \cdot A_i + \sum_{j=1}^{n+\hat{\ell}} n_j \cdot B_j,$$

where A_i and B_i are as in Definition 3.2. To see Equation (5.1), note that for $\mathcal{D} = A_i$ or B_j , we have $e(\mathcal{D}) + n_{\mathbf{x}}(\mathcal{D}) + n_{\mathbf{y}}(\mathcal{D}) = 2$, while each \mathcal{D} also has total weight 2 at the boundary. Equation (5.2) works similarly. \square

$$(5.3) \quad \delta^1(\mathbf{x}) = \sum_{\{\mathbf{y} \in \mathfrak{S}, B \in \mathcal{D}(\mathbf{x}, \mathbf{y}) \mid \mathbf{m}(B)=1\}} \# \widehat{m}^B(\mathbf{x}, \mathbf{y}) \cdot \widehat{b}(B) \cdot \otimes \mathbf{y}.$$

Proposition 5.3. *The sum appearing on the right in Equation (5.3) is finite.*

Proof. Given \mathbf{x}, \mathbf{y} , the set of $B \in \mathcal{D}(\mathbf{x}, \mathbf{y})$ with fixed $\mathbf{m}(B)$ is a finite set plus the addition of periodic domains. By admissibility, only finitely many of these elements have only positive local multiplicities. \square

Proposition 5.4. *The map δ^1 satisfies the curved type D structure relation, with curvature $\mu_0 = \sum_{\{r,s\} \in M} U_r U_s$.*

Proof. This works as in the proof of [9, Proposition 6.3], with a little modification. In this case, there are two additional types of possible boundary degenerations, ones that contain exactly one w_i marking and exactly one z_i marking. In fact, for each i , there are exactly two such boundary degenerations: one with α -boundary, and one with β -boundary. The contributions to $\delta^1 \circ \delta^1$ of these two boundary degenerations cancel. \square

Let $\hat{c}^* R(\mathcal{H}^\wedge, J)$ denote the curved type D structure defined above.

Proposition 5.5. *If J_0 and J_1 are any two generic almost-complex structures, there quasi-isomorphism of curved, graded type D structures over \hat{C}*

$$\hat{c}^* R(\mathcal{H}^\wedge, J_0) \simeq^{\hat{C}^*} R(\mathcal{H}^\wedge, J_1).$$

Proof. This follows exactly as in [9, Proposition 6.4]. \square

5.2. Middle diagrams. Fix a middle diagram

$$\mathcal{H}^\parallel = (\Sigma_0, (\check{Z}_1, \dots, \check{Z}_{2m}), (\hat{Z}_1, \dots, \hat{Z}_{2n}), \{\check{\alpha}_1, \dots, \check{\alpha}_{2m-1}\}, \{\hat{\alpha}_1, \dots, \hat{\alpha}_{2n-1}\}, \{\alpha_1^c, \dots, \alpha_g^c\}, \{\beta_1, \dots, \beta_{g+m+n+\ell_\parallel-1}\}, \{w_1, \dots, w_{\ell_\parallel}\}, \{z_1, \dots, z_{\ell_\parallel}\}).$$

Let M^\parallel be the induced β -matching as in Definition 3.7; and let \tilde{M} be a compatible matching on $\{1, \dots, 2m\}$, in the sense of Definition 3.9.

Definition 5.6. *Let \mathcal{H}^\parallel be a middle diagram, equipped with a matching \tilde{M} on the incoming boundary components. Let*

$$\check{C}(\mathcal{H}^\parallel) = \mathcal{C}(m) \otimes \mathbb{F}[w_1, z_1, \dots, w_{\ell_\parallel}, z_{\ell_\parallel}]; \quad \hat{C}(\mathcal{H}^\parallel) = \mathcal{C}(n) \otimes \mathbb{F}[w_1, z_1, \dots, w_{\ell_\parallel}, z_{\ell_\parallel}].$$

Our aim here is to define a curved type DA bimodule associated to the middle diagram, denoted $\hat{c}^* RQ(\mathcal{H}^\parallel)_{\check{C}^*}$.

Each middle Heegaard state \mathbf{x} determines two subsets

$$\check{\alpha}(\mathbf{x}) \subset \{1, \dots, 2m\} \quad \text{resp.} \quad \hat{\alpha}(\mathbf{x}) \subset \{1, \dots, 2n\}$$

consisting of those $i \in \{1, \dots, 2m\}$ resp. $\{1, \dots, 2n\}$ with $\mathbf{x} \cap \check{\alpha}_i \neq \emptyset$ resp $\mathbf{x} \cap \hat{\alpha}_i \neq \emptyset$. As an \mathbb{F} -vector space $RQ(\mathcal{H}^\parallel)$ is spanned by the middle Heegaard states of \mathcal{H}^\parallel . Let

$$\check{I}(\mathbf{x}) = \mathbf{I}_{\check{\alpha}(\mathbf{x})} \quad \text{and} \quad \hat{I}(\mathbf{x}) = \mathbf{I}_{\{1, \dots, 2n\} \setminus \hat{\alpha}(\mathbf{x})}.$$

The $I(n) - I(m)$ -bimodule structure is specified by

$$(5.4) \quad \hat{I}(\mathbf{x}) \cdot \mathbf{x} \cdot \check{I}(\mathbf{x}) = \mathbf{x}.$$

we need one more piece of data: an orientation \vec{W} on $W = W^\parallel \cup \vec{W}$. Each boundary component \check{Z}_i , \hat{Z}_j , w_i or z_i of \mathcal{H}^\parallel corresponds to some point on W .

Orient W from the w boundaries to the z boundaries. (We choose this convention to agree with [9]; it is opposite to the orientation on the link as specified in Section 3.1.) There are other components of W that connect various \hat{Z} -boundaries.

There are two kinds of \check{Z} boundaries in W^\parallel : those that are outwardly oriented in W^\parallel , and those that are inwardly oriented. Their corresponding orbits are called *even* and *odd* respectively; and this partition of the orbits into even and odd is called the \vec{W} -induced orbit marking. The terminal boundary of any component of W corresponds either to a \hat{Z} -boundary, or a z -boundary. To each boundary component in \check{Z}_i , which we think of as a point on \vec{W} , we associate an element z_j or \hat{Z}_j , which is the terminal point of the component of \vec{W} (with respect to its orientation) that contains \check{Z}_i . We denote this $\tau(\check{Z}_i)$.

Definition 5.7. Recall that a set of Reeb chords $\{\rho_1, \dots, \rho_j\}$ in $\check{\mathcal{H}}^\parallel$ is called algebraic if for any pair of distinct chords ρ_a and ρ_b ,

- the chords ρ_a and ρ_b are on different boundary components \hat{Z}_i and \hat{Z}_j ,
- the initial points ρ_a^- and ρ_b^- are on different α -curves; and
- the terminal points ρ_a^+ and ρ_b^+ are on different α -curves.

As explained in [9, Section 8.1], algebraic packets determine algebra elements.

Definition 5.8. Fix a Heegaard state \mathbf{x} and a sequence $\vec{a} = (a_1, \dots, a_\ell)$ of pure algebra elements of $\check{\mathcal{C}}(\mathcal{H}^\parallel)$. A sequence of constraint packets ρ_1, \dots, ρ_h is called (\mathbf{x}, \vec{a}) -compatible if there is a sequence $1 \leq k_1 < \dots < k_\ell \leq h$ so that the following conditions hold:

- the constraint packets ρ_{k_i} consist of chords in \check{Z} , and they are algebraic, in the sense of Definition 5.7,
- $\check{I}(\mathbf{x}) \cdot \check{b}(\rho_{k_1}) \otimes \dots \otimes \check{b}(\rho_{k_\ell}) = \mathbf{I}(\mathbf{x}) \cdot a_1 \otimes \dots \otimes a_\ell$, as elements of $RQ(\mathcal{H}^\vee) \otimes \check{\mathcal{C}}^{\otimes \ell}$
- for each $t \notin \{k_1, \dots, k_\ell\}$, the constraint packet ρ_t is one of the following types:
 - (DA ρ -1) it is a singleton set $\{o_i\}$, containing a single Reeb orbit o_i that covers the boundary component \check{Z}_i , which is *odd* for the \vec{W} -induced orbit marking.
 - (DA ρ -2) it consists of two elements $\{o_i, v_j\}$, where o_i is a Reeb orbit that covers a boundary component \check{Z}_i which is *even*, with $\{i, j\} \in M$, and where v_j is one of the two Reeb chords that covers \check{Z}_j with multiplicity one.
 - (DA ρ -3) it is of the form $\{o_k\}$, where o_k is the simple Reeb orbit around some component in \hat{Z}
 - (DA ρ -4) it is of the form $\{\rho_j\}$, where ρ_j is a Reeb chord of length $1/2$ supported in some \hat{Z} .

Let $\llbracket \mathbf{x}, a_1, \dots, a_\ell \rrbracket$ be the set of all sequences of constraint packets ρ_1, \dots, ρ_h that are (\mathbf{x}, \vec{a}) -compatible.

There is an algebra element $\hat{b}(B, \rho_1, \dots, \rho_h)$ defined as follows. We multiply $\hat{b}(B)$ (as defined in Definition 5.1) by a monomial in $\hat{\mathcal{C}}(\mathcal{H}^\parallel)$, determined as follows.

- For each packet $\rho_i = \{o_i\}$ of Type ((DA ρ -1)), multiply by the algebra element associated to the terminal point $\tau(\check{Z}_i)$. This terminal element $\tau(\check{Z}_i)$ can either be of the form \hat{Z}_j , in which case the algebra element is U_j ; or it can be some z_j , in which case the algebra element is z_j .

- For each packet ρ_i consisting of a single Reeb orbit that covers w_i or z_i , multiply by a factor of w_i resp. z_i respectively.

(In particular, the packets of Type (DA ρ -2) contribute a factor of 1.)

Proposition 5.9. *If \mathcal{H}^\parallel is admissible, for each $(\mathbf{x}, a_1, \dots, a_\ell)$, there are only finitely many choices of $(B, \rho_1, \dots, \rho_h)$ so that*

- $\text{ind}(B) = 1$.
- The domain B has only non-negative local multiplicities.
- $(\mathbf{x}, \rho_1, \dots, \rho_h)$ is $(\mathbf{x}, a_1, \dots, a_\ell)$ -compatible.

Proof. By the index requirement, the Δ -grading on the output element is determined by \mathbf{x} , \mathbf{y} , and (a_1, \dots, a_ℓ) . In particular, this gives an upper bound on the number of isolated odd orbits that are allowed among the ρ_1, \dots, ρ_h , and also on the total weight of B at \widehat{Z} .

If both B and B' represent actions of $(\mathbf{x}, a_1, \dots, a_\ell)$ with output $b \otimes \mathbf{y}$; and suppose that they have the same number of odd orbits. Then, $B - B'$ is a periodic domain, in the sense of Definition 3.8. Finiteness is now ensured by admissibility. \square

Definition 5.10. *Fix the following data:*

- an admissible middle diagram \mathcal{H}^\parallel with matching M^\parallel , with induced one-manifold W^\parallel
- a compatible matching \widetilde{M} , with induced one-manifold \widetilde{W}
- an orientation \vec{W} on the one-manifold $W = W^\parallel \cup \widetilde{W}$.
- a compatible almost-complex structure J on \mathcal{H}^\parallel .

We abbreviate this data $(\mathcal{H}^\parallel, \widetilde{M}, \vec{W}, J)$. Let RQ be the associated $I(n) - I(m)$ -bimodule structure as specified in Equation (5.4). For all $k \geq 0$, define maps $\delta_k^1: RQ \otimes \check{C}^{\otimes k} \rightarrow RQ$ by

$$(5.5) \quad \delta_{k+1}^1(\mathbf{x}, a_1, \dots, a_k) = \sum_{\substack{\mathbf{y} \in \mathfrak{S} \\ (\rho_1, \dots, \rho_h) \in \llbracket \mathbf{x}, a_1, \dots, a_k \rrbracket \\ B \in \pi_2(\mathbf{x}, \rho_1, \dots, \rho_h, \mathbf{y}) \mid \text{ind}(B, \rho_1, \dots, \rho_h) = 1}} \# \widehat{M}(\mathbf{x}, \mathbf{y}, \rho_1, \dots, \rho_h) \cdot \widehat{b}(B, \rho_1, \dots, \rho_h) \otimes \mathbf{y}.$$

The sums in the above map are finite by Proposition 5.9.

Proposition 5.11. *Let $(\mathcal{H}^\parallel, \widetilde{M}, \vec{W}, J)$ be the data required to define RQ , as in Definition 5.10. The $I(2n) - I(2m)$ -bimodule $RQ(\mathcal{H}^\parallel)$, equipped the operations*

$$\delta_{\ell+1}^1: RQ(\mathcal{H}^\parallel) \otimes \check{C}^{\otimes \ell} \rightarrow \widehat{C} \otimes RQ(\mathcal{H}^\parallel)$$

defined above endows $RQ(\mathcal{H}^\parallel)$ with the structure of a curved $\mathcal{C}(n, \widehat{M}) - \mathcal{C}(m, M)$ DA bimodule, where \widehat{M} is the matching on $\{1, \dots, 2n\}$ induced by M^\parallel and M . This bimodule is also strictly unital and bounded. Moreover, for any two generic choices of J , the resulting curved DA bimodules are homotopy equivalent.

Proof. The verification of the curved DA bimodule relations follows as in [9, Proposition 10.10]. The key novelty is that now there are α -boundary degenerations. contribute terms of $w_i z_i \otimes \mathbf{x}$ to $\delta_1^1 \circ \delta_1^1(\mathbf{x})$. These cancel with the analogous terms coming from the β -boundary degenerations containing the basepoints w_i .

Strict unitality is obvious from the construction. Boundedness follows once again from admissibility.

Varying J induces homotopy equivalences by the usual continuation principle; compare for example [9, Section 8.3]. \square

Let $\hat{c}^* RQ(\mathcal{H}^\parallel)_{\check{c}^*}$ denote the curved type DA bimodule associated to \mathcal{H}^\parallel by the above procedure.

Remark 5.12. *The DA bimodule depends on the data $(\mathcal{H}^\parallel, \widetilde{M}, \vec{W}, J)$. The above theorem shows that its homotopy type is independent of the choice of J . The dependence on \widetilde{M} is crucial. One could investigate its independence of the orientation \vec{W} , but we do not need that in the sequel. Nonetheless, to shorten notation, we write simply $\hat{c}^* RQ(\mathcal{H}^\parallel)_{\check{c}^*}$.*

5.3. The pairing theorem.

Definition 5.13. *Fix the following:*

- an marked upper diagram \mathcal{H}^\wedge
- an marked middle diagram \mathcal{H}^\parallel
- an identification $\partial\mathcal{H}^\wedge \cong \check{\partial}\mathcal{H}^\parallel$.

This is called compatibly gluable if the matching M^\parallel is compatible with the matching on $\check{\partial}\mathcal{H}^\parallel$ induced by \mathcal{H}^\wedge and the above identification. Given boundary-identified diagrams \mathcal{H}^\parallel and \mathcal{H}^\wedge , their gluing $\mathcal{H}^\parallel \cup_{\check{\partial}\mathcal{H}^\parallel \cong \partial\mathcal{H}^\wedge} \mathcal{H}^\wedge$ is naturally an upper diagram.

If \mathcal{H}^\parallel and \mathcal{H}^\wedge are admissible, their gluing is also admissible.

If $(\mathcal{H}^\parallel, \mathcal{H}^\wedge, \partial\mathcal{H}^\wedge \cong \check{\partial}\mathcal{H}^\parallel)$ is compatibly gluable, there is a one-to-one correspondence between pairs of states \mathbf{x} and \mathbf{y} , where \mathbf{x} is an partial Heegaard state for \mathcal{H}^\parallel and \mathbf{y} is an upper Heegaard state for \mathcal{H}^\wedge , and $\alpha(\mathbf{x}) = \{1, \dots, 2n\} \setminus \hat{\alpha}(\mathbf{y})$.

We have the following straightforward adaptation of the pairing theorem from [9, Theorem 10.11] (compare also [3, Theorem 11]):

Theorem 5.14. *Fix compatibly gluable diagrams $(\mathcal{H}^\wedge, \mathcal{H}^\parallel, \check{\partial}\mathcal{H}^\parallel \cong \partial\mathcal{H}^\wedge)$, where \mathcal{H}^\wedge and \mathcal{H}^\parallel are admissible. Let $C_1 = C(\mathcal{H}^\wedge) = \check{C}(\mathcal{H}^\parallel)$; $C_2 = \hat{C}(\mathcal{H}^\parallel)$.*

Under the above hypotheses, there is a quasi-isomorphism of curved type D structures

$${}^{C_2}R(\mathcal{H}^\parallel \# \mathcal{H}^\wedge) \simeq {}^{C_2}RQ(\mathcal{H}^\parallel)_{C_1} \boxtimes {}^{C_1}R(\mathcal{H}^\wedge).$$

Proof. The proof of [9, Theorem 10.11] applies, after a few observations. Recall that in that earlier result, the tensor product is a curved type D structure, with curvature $\sum_{\{i,j\} \in M} U_i U_j$. The curvature term comes from β -boundary degenerations. The arguments from that proof also give rise to additional curvature terms $\sum_i w_i z_i$;

but (as in the case of Proposition 5.4) these terms are cancelled by α -boundary degenerations. \square

5.4. Extending diagrams. Fix the data $(\mathcal{H}^\parallel, \vec{M}, \vec{W}, J)$ as in Definition 5.10 required to form the type DA bimodule $\hat{C}RQ(\mathcal{H}^\parallel)_{\hat{C}}$

Let \mathcal{H}^\parallel be a marked middle diagram, and let $\mathcal{H}^{\parallel,x}$ be an extended marked diagram as in Definition 3.11.

Define maps

$$\delta_{1+k}^1: RQ^x(\mathcal{H}^{\parallel,x}) \otimes \check{B}^{\otimes k} \rightarrow \hat{B} \otimes RQ^x(\mathcal{H}^{\parallel,x}).$$

in the obvious way.

Let $\check{\iota}: \check{C} \rightarrow \check{B}$ and $\hat{\iota}: \hat{C} \rightarrow \hat{B}$ be the natural inclusion maps.

Proposition 5.15. *Fix the data $(\mathcal{H}^\parallel, \vec{M}, \vec{W}, J)$ as in Definition 5.10 required to form the type DA bimodule $\hat{C}RQ(\mathcal{H}^\parallel)_{\hat{C}}$, and let $\mathcal{H}^{\parallel,x}$ be an extension of \mathcal{H}^\parallel . The type DA bimodules associated to \mathcal{H}^\parallel and $\mathcal{H}^{\parallel,x}$ are related by the formula*

$$\hat{B}[\iota]_{\hat{C}} \boxtimes^{\hat{C}} RQ(\mathcal{H}^\parallel)_{\hat{C}} = \hat{B} RQ_{\check{B}}^x(\mathcal{H}^{\parallel,x}) \boxtimes^{\check{B}} [\iota]_{\check{C}}.$$

Proof. The proof is exactly as in the unmarked case [9, Proposition 11.1]. \square

5.5. Specializing to $w_i = z_i = 0$. Of course, all of the constructions described above can also be specialized to $w_i = z_i = 0$ for all i . The resulting modules are denoted $\widehat{R}(\mathcal{H}^\wedge)$, $\widehat{RQ}(\mathcal{H}^\parallel)$, and $\widehat{Q}(\mathcal{H}^\vee)$; they are defined over the algebras where $w_i = z_i = 0$; e.g. if \mathcal{H}^\parallel has $2m$ inputs and $2n$ outputs, then

$$\widehat{RQ}(\mathcal{H}^\parallel) = {}^{C(n)}\widehat{RQ}(\mathcal{H}^\parallel)_{C(m)}.$$

Explicitly, the holomorphic disks that contribute in the differential of \widehat{RQ} are required to have vanishing local multiplicity at all w_i and z_i ; and moreover, they never count isolated orbits. (Isolated even orbits were not counted for RQ ; isolated odd orbits as in Definition 5.8 (DA ρ -1) contribute w_i factors in RQ , but we have set $w_i = 0$ here.)

The above results can be readily specialized to this blocked theory.

For example, we can define $\widehat{RQ}^x(\mathcal{H}^{\parallel,x})$ to be the $w = z = 0$ specialization of $RQ^x(\mathcal{H}^{\parallel,x})$. Proposition 5.15 implies then that

$${}^{B(n)}[\iota]_{C(n)} \boxtimes^{C(n)} \widehat{RQ}(\mathcal{H}^\parallel)_{C(m)} = {}^{B(n)}\widehat{RQ}_{B(m)}^x(\mathcal{H}^{\parallel,x}) \boxtimes^{B(m)} [\iota]_{C(m)}.$$

Also, Theorem 5.14 has the following specialization:

Theorem 5.16. *Fix compatibly gluable diagrams $(\mathcal{H}^\wedge, \mathcal{H}^\parallel, \check{\partial}\mathcal{H}^\parallel \cong \partial\mathcal{H}^\wedge)$, where \mathcal{H}^\wedge and \mathcal{H}^\parallel are admissible, where Let $C_1 = C(m)$; $C_2 = C(n)$, provided that \mathcal{H}^\parallel has $2m$ incoming boundary circles and $2n$ outgoing ones. There is a quasi-isomorphism of curved type D structures*

$${}^{C_2}\widehat{R}(\mathcal{H}^\parallel \# \mathcal{H}^\wedge) \simeq {}^{C_2}\widehat{RQ}(\mathcal{H}^\parallel)_{C_1} \boxtimes^{C_1} \widehat{R}(\mathcal{H}^\wedge),$$

Proof. This follows immediately from Theorem 5.14, after setting $w_i = z_i = 0$. \square

6. MODULES FOR A MARKED MINIMUM

Our aim here is to define algebraically type DA bimodules. These will come in two versions:

- ${}^{\mathcal{B}(n)}\widehat{V}_{\mathcal{B}(n+1)}$
- ${}^{\mathcal{B}(n)}V_{\mathcal{B}(n+1)}$ with base ring $\mathbb{F}[w, z]$, whose $w = z = 0$ specialization is the above module.

These will be used to define also curved variants ${}^{\mathcal{B}_2^*}\widehat{V}_{\mathcal{B}_1^*}$ and ${}^{\mathcal{B}_2^*}V_{\mathcal{B}_1^*}$ (cf. Proposition 6.4).

We shall also define another module ${}^{\mathcal{A}'_1}V'_{\mathcal{A}'_2}$ with the property that

$${}^{\mathcal{B}_2^*}V'_{\mathcal{B}_1^*} \boxtimes^{\mathcal{B}_1^*, \mathcal{A}'_1} \mathcal{K} \simeq {}^{\mathcal{A}'_1}V'_{\mathcal{A}'_2} \boxtimes^{\mathcal{A}'_2, \mathcal{B}_2^*} \mathcal{K}$$

(cf. Proposition 6.5).

Their relationship with the holomorphically defined modules will be established in Section 7.

6.1. Modules in the algebraically specialized case. Consider the subring $I_{\geq k} \subset I(n+1)$ of the idempotent ring of $\mathcal{B}(n+1)$.

Let M be a matching on $\{1, \dots, 2n+2\}$ with $\{1, 2\} \in M$. Let M' be the corresponding matching on $\{1, \dots, 2n\}$ with $\{i, j\} \in M'$ if and only if $\{i+2, j+2\} \in M$.

The idempotent states \mathbf{x} for $\mathcal{B}_1 = \mathcal{B}(n+1)$ are called *preferred* if

$$1 \leq |\mathbf{x} \cap \{0, 1, 2\}| \leq 2 \quad \text{and} \quad \mathbf{x} \neq \{0, 1\}$$

Given a preferred idempotent state \mathbf{x} for \mathcal{B}_1 , the corresponding idempotent $\psi(\mathbf{x})$ for $\mathcal{B}(n) = \mathcal{B}_2$ contains 0 precisely when $|\mathbf{x} \cap \{0, 1, 2\}| = 2$; and for $i > 0$, $i \in \psi(\mathbf{x})$ precisely when $i+2 \in \mathbf{x}$.

We construct now a type DA bimodule ${}^{\mathcal{B}(n)}\widehat{V}_{\mathcal{B}(n+1)}$, as follows.

As a right $I(n+1)$ -module, \widehat{V} splits as a direct sum of six modules

$$X_0 \oplus X_1 \oplus X_2 \oplus Y_0 \oplus Y_1 \oplus Y_2,$$

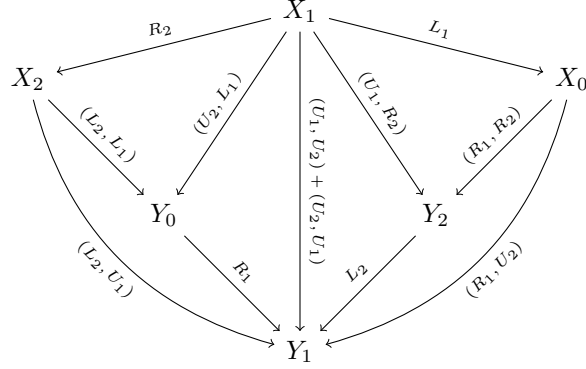
where $X_i \cong Y_i$ is generated by the preferred idempotents in $I_{\geq i}$. The left $I(n)$ -module action is specified by

$$X \cdot \mathbf{I}_{\mathbf{x}} = \mathbf{I}_{\psi(\mathbf{x})} \cdot X \cdot \mathbf{I}_{\mathbf{x}}$$

for any $X \in \widehat{V}$.

For example, X_0 splits naturally into two summands, according to the whether or not 0 appears in the left idempotent: a summand where 0 appears in the left idempotent and both 0 and 2 (but not 1) appear in the right idempotent; another one where 0 does not appear in the left idempotent and 0 (but not 1 or 2) appears in the right idempotent.

The action by $\mathcal{B}(n+1)$ is specified using Figure 12. That figure appears to specify a bimodule with incoming algebra $\mathcal{B}(1)$ and outgoing algebra $\mathcal{B}(0)$. We extend this to a bimodule ${}^{\mathcal{B}(n, M')}\widehat{V}_{\mathcal{B}(n+1, M)}$ as follows.

FIGURE 12. Actions on \widehat{V}

If $b = \mathbf{I}_x \cdot b \cdot \mathbf{I}_y \in I_{\geq 1} \cdot \mathcal{B}(n+1) \cdot I_{\geq 1}$ has $\mathbf{w}_1(b) = \mathbf{w}_2(b) = 0$, then let $\Psi(b) = b'$ denote the algebra element $b' = \mathbf{I}_{\psi(x)} \cdot b' \cdot \mathbf{I}_{\psi(y)}$ with $\mathbf{w}_i(b') = \mathbf{w}_{i+2}(b)$. Define $\Psi(b)$ similarly for $b \in I_{\geq 2} \cdot \mathcal{B}(n+1) \cdot I_{\geq 2}$.

For the extension, define $\delta_2^1(X, b) = \Psi(b) \otimes X$ for all $X \in \widehat{V}$. The arrows above are similarly extended; e.g.

$$\delta_3^1(X_2, L_2 b_1, L_1 b_2) = \Psi(b_1) \cdot \Psi(b_2) \otimes Y_0.$$

In particular, $\delta_k^1 \equiv 0$ for $k \geq 4$.

Definition 6.1. Let \mathcal{A}, \mathcal{B} be algebras and ${}^{\mathcal{B}}X_{\mathcal{A}}$ a type DA bimodule. Fix $a \in \mathcal{A}$ and $b \in \mathcal{B}$. We say that X is a - b -equivariant if the following conditions hold:

- $\delta_1^1(x, a) = b \otimes x$ for all $x \in X$
- $\delta_{k+1}^1(x, a_1, \dots, a_k) = 0$ if for all $k > 1$ if $a_i = a$ for some i .

We say that X is annihilated by a if X is a -0-equivariant.

Proposition 6.2. The object ${}^{\mathcal{B}_2}\widehat{V}_{\mathcal{B}_1}$ is a type DA bimodule, which is $U_r \cdot U_s$ - $U_{r+2}U_{s+2}$ equivariant for all $r, s \in \{1, \dots, 2n\}$; and which is annihilated by U_1U_2 .

Proof. These are straightforward computations. \square

6.2. The algebraically unspecialized case. We can extend ${}^{\mathcal{B}_2}\widehat{V}_{\mathcal{B}_1}$ to a module ${}^{\mathcal{B}_2}V_{\mathcal{B}_1}$ over $\mathbb{F}[w, z]$. Generators for the module are the same as before, but now actions are specified in the following diagram, where k, ℓ are arbitrary non-negative

integers.

(6.1)

The arrows are to be interpreted as before; e.g.

$$\delta_3^1(X_2, L_2U_2 \cdot b_1, L_1U_1^2) = w^2z \cdot \Psi(b_1) \cdot \Psi(b_2) \otimes Y_0.$$

Again, $\delta_k^1 \equiv 0$ for $k \geq 4$.

Proposition 6.3. *The object $\mathcal{B}_2[w, z]V_{\mathcal{B}_1}$ is a type DA bimodule, which is annihilated by U_1U_2 , and which is $U_rU_s - U_{r+2}U_{s+2}$ -equivariant for all $r, s \in \{1, \dots, 2n\}$. Specializing V to $w = z = 0$ gives $\mathcal{B}_2\widehat{V}_{\mathcal{B}_1}$.*

6.3. Curved modules. Fix any matching M_2 on $\{1, \dots, 2n\}$, and let M_1 be the matching matching on $\{1, \dots, 2n+2\}$ specified as follows:

- $\{1, 2\} \in M_1$
- For all $i, j \in \{1, \dots, 2n\}$, $\{i, j\} \in M_2 \iff \{i+2, j+2\} \in M_1$.

Let $\mathcal{B}_1^* = \mathcal{B}^*(n+1, M_1)$, $\mathcal{B}_2^* = \mathcal{B}^*(n, M_2)$, and $\mathcal{B}_2^*[w, z]$ denote \mathcal{B}_2^* where the algebra is extended by two additional variables w and z .

Proposition 6.4. For \mathcal{B}_1^* and \mathcal{B}_2^* as above, the operations δ_{1+k}^1 endow $\mathcal{B}_2^* \widehat{V}_{\mathcal{B}_1^*}$ the structure of a curved type DA bimodule. More generally, the operations specified above $\mathcal{B}_2^{*[w,z]} V_{\mathcal{B}_1^*}$ is a curved DA bimodule, whose $w = z = 0$ specialization is \widehat{V} .

Proof. Proposition 6.2 ensures that \widehat{V} is $\mu_0^{M_1} - \mu_0^{M_2}$ -equivariant type DA bimodule. But such a bimodule is simply a curved type DA bimodule. For V , the result follows from Proposition 6.3. \square

6.4. Commuting with the canonical bimodule. Let $\mathcal{A}_1'' = \mathcal{A}''(n+1, M_1)$ and $\mathcal{A}_2'' = \mathcal{A}''(n, M_2)$, with M_1 and M_2 as in Section 6.3. Our aim here is to construct a type DA bimodule $\mathcal{A}_1'' V'_{\mathcal{A}_2''}$ which is dual to V .

As a left $I_{2n+2, n+2}$ module V' splits into summands

$$(6.2) \quad V' = X'_0 \oplus X'_1 \oplus X'_2 \oplus Y'_0 \oplus Y'_1 \oplus Y'_2,$$

called *types*; where the idempotents of each summand is complementary to the corresponding summand in V ; i.e.

$$\begin{aligned} X'_1 &= X'_{\{0,2\}} \oplus X'_0 & X'_0 &= X'_{\{1,2\}} \oplus X'_{\{1\}} & X'_2 &= X'_{\{0,1\}} \\ Y'_0 &= Y'_{\{1,2\}} \oplus Y'_{\{1\}} & Y'_1 &= Y'_{\{0\}} \oplus Y'_{\{0,2\}} & Y'_2 &= Y'_{\{0,1\}} \end{aligned}$$

where here the subscript indicates the idempotents; e.g. as a left $I(2n+2, n+2)$ -module, we have

$$X'_{\{1,2\}} \cong I(2n+2, n+2) \cdot \left(\sum_{\{\mathbf{x} \mid \mathbf{x} \cap \{0,1,2\} = \{1,2\}\}} \mathbf{I}_{\mathbf{x}} \right).$$

Idempotent states \mathbf{x} for \mathcal{A}'' are called *preferred* if

$$1 \leq |\mathbf{x} \cap \{0, 1, 2\}| \leq 2$$

Given a preferred idempotent state \mathbf{x} for $\mathcal{B}_1(2n+2, n+2)$, there is a corresponding idempotent $\varphi(\mathbf{x})$ for $\mathcal{B}(2n, n+1)$, which contains 0 precisely when $|\mathbf{x} \cap \{0, 1, 2\}| = 2$; and for $i > 0$, $i \in \varphi(\mathbf{x})$ precisely when $i+2 \in \mathbf{x}$. The bimodule structure is now specified by requiring

$$\mathbf{I}_{\mathbf{x}} \cdot P = P \cdot \mathbf{I}_{\varphi(\mathbf{x})}.$$

Define

$$\delta_1^1: V' \rightarrow \mathcal{A}_1'' \otimes V'$$

as in Figure 13.

Define

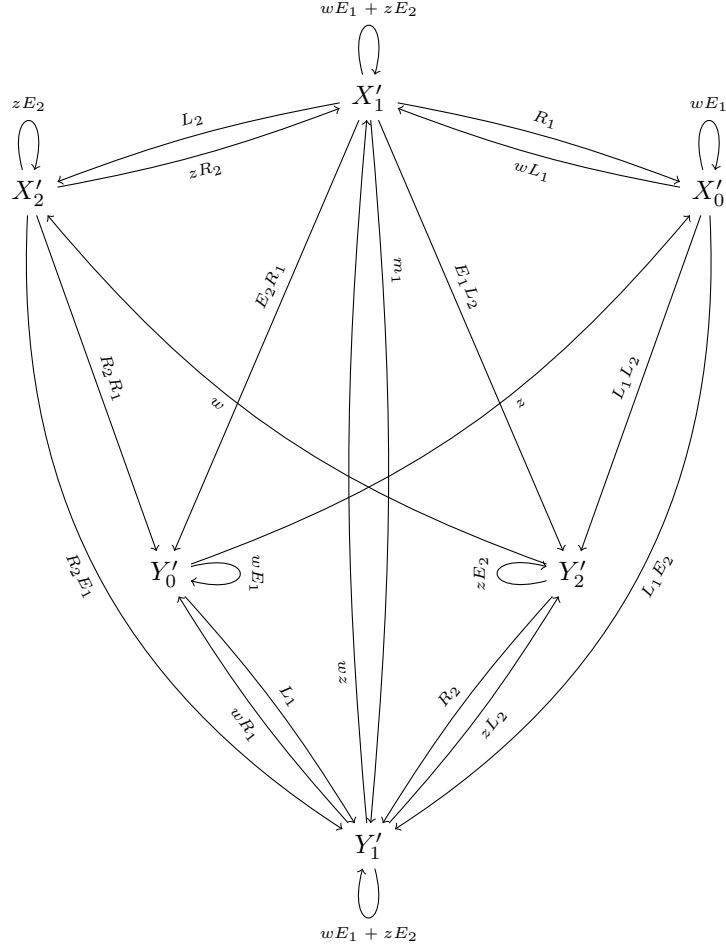
$$\delta_2^1: V' \otimes \mathcal{A}_2'' \rightarrow \mathcal{A}_1'' \otimes V'$$

as follows. Given $P \in V$ in one of the six summands from Equation (6.2), with $P = \mathbf{I}_{\mathbf{x}} \cdot P$, and given $b = \mathbf{I}_{\varphi(\mathbf{x})} \cdot b \cdot \mathbf{I}_{\mathbf{y}} \in \mathcal{B}(2n, n+1) \subset \mathcal{A}_2''$, let $\Phi(b) = b' \in \mathcal{B}(2n+2, n+2) \subset \mathcal{A}_1''$ be the algebra element $b' = \mathbf{I}_{\mathbf{x}} \cdot b' \cdot \mathbf{I}_{\mathbf{y}}$ with weight $\omega_i(b') = \omega_{i-2}(b)$ and $\omega_0(b') = \omega_1(b)$. Then,

$$\delta_2^1(X, b) = \Phi(b) \cdot P',$$

where $P' = \mathbf{I}_{\mathbf{y}} \cdot P'$ is in the same type as X . We extend this to an action of all of \mathcal{A}_2'' by requiring

$$\delta_2^1(X, E_i \cdot b) = E_{i+2} \cdot \delta_2^1(X, b).$$

FIGURE 13. Specifying δ_1^1 in V'

Proposition 6.5. *The operations give V' the structure of a type DA bimodule $\mathcal{A}_1'' V' \mathcal{A}_2''$. This bimodule is related to $\mathcal{B}_2^* V_{\mathcal{B}_1^*}$ by the identity*

$$\mathcal{A}_1'' V' \mathcal{A}_2'' \boxtimes \mathcal{A}_2'', \mathcal{B}_2^* \mathcal{K} \simeq \mathcal{A}_2'' V_{\mathcal{A}_1''} \boxtimes \mathcal{A}_1'', \mathcal{B}_1^* \mathcal{K};$$

similarly,

$$\mathcal{A}_1'' \widehat{V}'_{\mathcal{A}_2''} \boxtimes \mathcal{A}_2'', \mathcal{B}_2^* \mathcal{K} \simeq \mathcal{A}_2'' \widehat{V}_{\mathcal{A}_1''} \boxtimes \mathcal{A}_1'', \mathcal{B}_1^* \mathcal{K}.$$

Proof. These are all straightforward computations. □

7. HOLOMORPHIC COMPUTATIONS

The diagram in Figure 14 shows a Heegaard diagram for a marked minimum. The left portion of this diagram (redrawn on the left in Figure 15) is stabilized as shown on the right in Figure 15. Rather than working directly with this diagram, we will

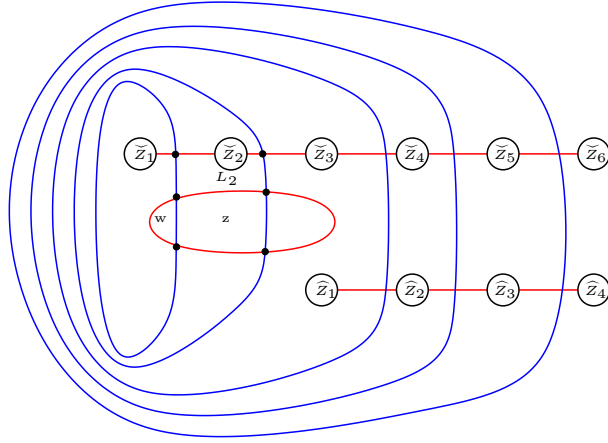


FIGURE 14. Heegaard diagram for a marked minimum.

find it convenient to work with the isotopic diagram shown in Figure 16. Since these diagrams are isotopic (and both are admissible), it follows that their associated type DA bimodules are homotopy equivalent. (This homotopy equivalence can be constructed by a continuation map, similar to the proof of J -invariance in Proposition 5.11.) We denote this latter diagram $\mathcal{H}^{\parallel, x}$.

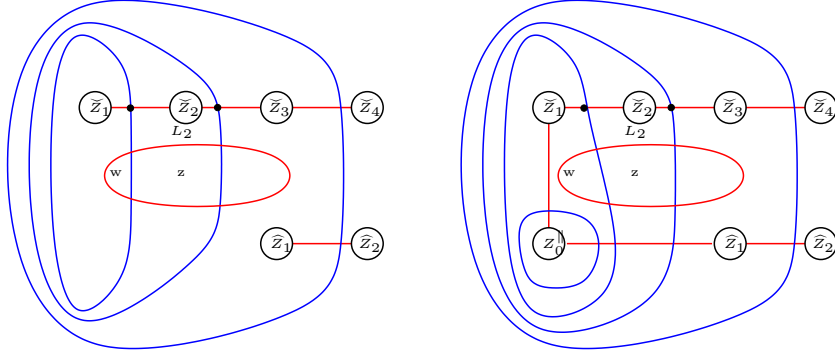


FIGURE 15. Heegaard diagram for a marked minimum.

After making some conformal choices, compute enough of that bimodule to compute the associated type DD -bimodule ${}^{\mathcal{B}_2^*}RQ^x(\mathcal{H}^{\parallel, e})_{\mathcal{B}_1^*} \boxtimes^{\mathcal{B}_1, \mathcal{A}''} \mathcal{K}$. Indeed, the main result of this section is the following

Proposition 7.1. *For a suitable choice of almost-complex structure on $\mathcal{H}^{\parallel, e}$, there is an identification ${}^{\mathcal{B}_2^*}RQ^x(\mathcal{H}^{\parallel, x})_{\mathcal{B}_1^*} \boxtimes^{\mathcal{B}_1^*, \mathcal{A}''} \mathcal{K} \simeq {}^{\mathcal{B}_2^*}V_{\mathcal{B}_1^*} \boxtimes^{\mathcal{B}_1^*, \mathcal{A}''} \mathcal{K}$, where V is the algebraically defined bimodule constructed in Section 6.*

Before turning to the proof, we make a few notational remarks about the statement. Note that $\mathcal{H}^{\parallel, x}$ is an extended diagram with $\ell = 1$, so its output algebra is $\mathcal{C}(n) \otimes \mathbb{F}[w_1, z_1]$. Correspondingly, the output algebra V as defined in Section 6 was $\mathcal{C}(n) \otimes \mathbb{F}[w, z]$. In the above identification of modules, we are using an isomorphism of algebras identifying w_1 and z_1 with w and z respectively.

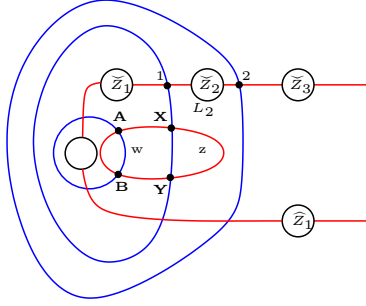


FIGURE 16. Heegaard diagram for a marked minimum.

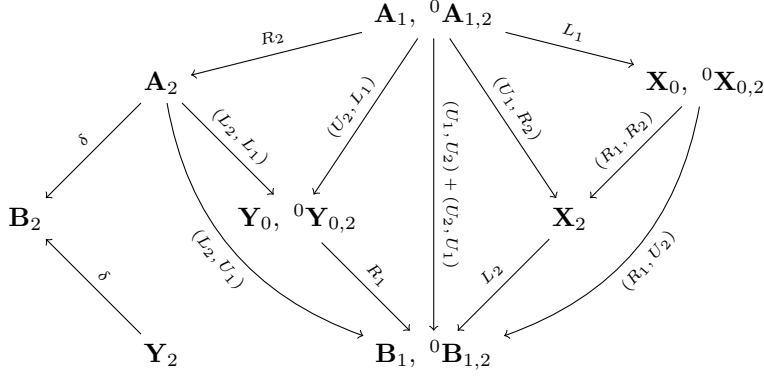


FIGURE 17. Some actions on $\widehat{RQ}^x(\mathcal{H}^{\parallel, x})$

7.1. **The blocked case.** In this section, we prove the following variant of Proposition 7.1, specialized to $w = z = 0$. (Note that this special case is sufficient to compute \widehat{HFL} for links which, in turn, determines the Thurston polytope of the underlying link.)

Proposition 7.2. *For a suitable choice of almost-complex structure on $\mathcal{H}^{\parallel, \epsilon}$, there is a homotopy equivalence*

$$(7.1) \quad \left(\frac{\beta_2 RQ^x(\mathcal{H}^{\parallel, \epsilon})_{\beta_1}}{w = z = 0} \right) \boxtimes^{\beta_1, \mathcal{A}'_1} \mathcal{K} \simeq^{\beta_2} \widehat{V}_{\beta_1} \boxtimes^{\beta_1, \mathcal{A}'_1} \mathcal{K}.$$

Proof. Our aim here is to prove this specialization here. First note that there are 12 generator types locally. We denote them

$$\begin{array}{cccccc} \mathbf{X}_2 & \mathbf{Y}_2 & {}^0\mathbf{X}_{0,2} & {}^0\mathbf{Y}_{0,2} & \mathbf{A}_2 & \\ \mathbf{B}_2 & \mathbf{A}_1 & \mathbf{B}_1 & {}^0\mathbf{A}_{1,2} & {}^0\mathbf{B}_{1,2} & \end{array}$$

We claim there is an almost-complex structure for which the moduli has the actions displayed in in Figure 12. (In that figure, arrows labelled by δ represent δ_1^1 actions.) Moreover, we show that there are no other actions starting at \mathbf{Y}_2 or \mathbf{B}_2 ; i.e. \mathbf{Y}_2 and \mathbf{B}_2 generate a type DA submodule.

To this end, label the domains in the Heegaard diagram as shown in Figure 18.

The rectangle \mathcal{D}_3 represents the differential

$$\mathbf{Y}_2 \xrightarrow[\mathcal{D}_3]{\delta} \mathbf{B}_2.$$

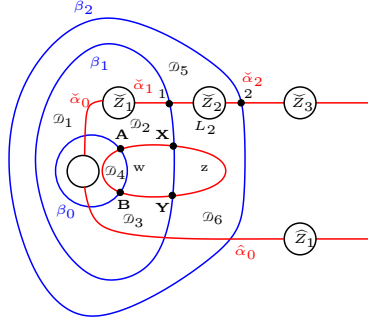


FIGURE 18. **Heegaard diagram for a marked minimum.** We have labelled various domains.

We now consider the differential that connect the various other generator types. There are the following polygons:

$$\begin{array}{ccccccc} \mathbf{A} & \xrightarrow[\mathcal{D}_4]{\delta} & \mathbf{B}, & \mathbf{A} & \xrightarrow[\mathcal{D}_2]{L_1} & \mathbf{X}, & \mathbf{X}_2 & \xrightarrow[\mathcal{D}_3+\mathcal{D}_6]{L_2} & \mathbf{B}_1 & \mathbf{A}_1 & \xrightarrow[\mathcal{D}_5]{R_2} & \mathbf{A}_2 \\ \mathbf{A}_2 & \xrightarrow[\mathcal{D}_2+\mathcal{D}_6]{(L_2, L_1)} & \mathbf{Y}_0, & \mathbf{X}_0 & \xrightarrow[\mathcal{D}_1+\mathcal{D}_5]{(R_1, R_2)} & \mathbf{X}_2, & \mathbf{Y}_0 & \xrightarrow[\mathcal{D}_1+\mathcal{D}_5]{(R_1, R_2)} & \mathbf{Y}_2, & \mathbf{A}_1 & \xrightarrow[\mathcal{D}_1+\mathcal{D}_2+\mathcal{D}_5]{(U_1, R_2)} & \mathbf{X}_2 \end{array}$$

We also have the following annuli that have holomorphic representatives:

$$\begin{array}{ccccccc} \mathbf{A}_2 & \xrightarrow[\mathcal{D}_1+\mathcal{D}_2+\mathcal{D}_3+\mathcal{D}_6]{(L_2, U_1)} & \mathbf{B}_1, & \mathbf{A}_1 & \xrightarrow[\mathcal{D}_2+\mathcal{D}_5+\mathcal{D}_6]{(U_2, L_1)} & \mathbf{Y}_0, & \mathbf{X}_0 & \xrightarrow[\mathcal{D}_1+\mathcal{D}_3+\mathcal{D}_5+\mathcal{D}_6]{(R_1, U_2)} & \mathbf{B}_1 \\ \mathbf{A}_1 & \xrightarrow[\mathcal{D}_1+\mathcal{D}_2+\mathcal{D}_3+\mathcal{D}_5+\mathcal{D}_6]{(U_1, U_2)} & \mathbf{B}_1 & \mathbf{A}_1 & \xrightarrow[\mathcal{D}_1+\mathcal{D}_2+\mathcal{D}_3+\mathcal{D}_5+\mathcal{D}_6]{(U_2, U_1)} & \mathbf{B}_1 & & & \end{array}$$

The latter two relations force also another arrow

$$\mathbf{A}_1 \xrightarrow[\mathcal{D}_1+\mathcal{D}_2+\mathcal{D}_3+\mathcal{D}_5+\mathcal{D}_6]{\delta} \mathbf{B}_1$$

which cancels against the δ induced by the bigon \mathcal{D}_4 . To see how, we consider the one-dimensional moduli space \mathcal{M} of holomorphic maps from \mathbf{A}_1 to \mathbf{B}_1 with the following properties:

- The map has shadow $\mathcal{D}_1 + \mathcal{D}_2 + \mathcal{D}_3 + \mathcal{D}_5 + \mathcal{D}_6$.
- The source has two punctures p_1 and p_2 , marked by the Reeb orbit o_1 and a length one Reeb chord covering \tilde{Z}_2 respectively.
- $t(p_1) > t(p_2)$.

The space \mathcal{M} has an end which corresponds to the arrow \mathbf{A}_1 to \mathbf{B}_1 with algebra element (U_1, U_2) (i.e. where p_1 goes to the boundary). In principle, it could have another end which is a broken flowline. One of those components must contain a puncture p_1 marked by o_1 (and no other punctures). But there evidently possible such shadow in the picture. It follows that \mathcal{M} has an odd number of ends where $t(p_1) = t(p_2)$. But these are exactly terms counted in δ_1^1 .

We choose an almost-complex structure which is sufficiently stretched out normal to β_2 . For such a choice of almost-complex structures, the analogous annuli also have holomorphic representatives:

$$\begin{array}{ccc} {}^0\mathbf{A}_{1,2} & \xrightarrow[\mathcal{D}_2+\mathcal{D}_5+\mathcal{D}_6]{(U_2, L_1)} & {}^0\mathbf{Y}_{0,2}, \quad {}^0\mathbf{X}_{0,2} \xrightarrow[\mathcal{D}_1+\mathcal{D}_3+\mathcal{D}_5+\mathcal{D}_6]{(R_1, U_2)} & {}^0\mathbf{B}_{1,2} \\ {}^0\mathbf{A}_{1,2} & \xrightarrow[\mathcal{D}_1+\mathcal{D}_2+\mathcal{D}_3+\mathcal{D}_5+\mathcal{D}_6]{(U_1, U_2)} & \mathbf{B}_{1,2} & \quad {}^0\mathbf{A}_{1,2} \xrightarrow[\mathcal{D}_1+\mathcal{D}_2+\mathcal{D}_3+\mathcal{D}_5+\mathcal{D}_6]{(U_2, U_1)} & {}^0\mathbf{B}_{1,2}. \end{array}$$

which also forces

$${}^0\mathbf{A}_{1,2} \xrightarrow[\mathcal{D}_1+\mathcal{D}_2+\mathcal{D}_3+\mathcal{D}_5+\mathcal{D}_6]{\delta} {}^0\mathbf{B}_{1,2}$$

We have verified the differentials from Figure 18. To verify that \mathbf{Y}_2 and \mathbf{B}_2 represent a submodule, we argue as follows. First, note that there are no positive domains that leave the generator type \mathbf{B} ; and indeed there are no positive domains leaving \mathbf{B}_2 going to \mathbf{B}_1 . Moreover, a positive domain leaving \mathbf{Y} must contain \mathcal{D}_3 . It must then either be simply \mathcal{D}_3 , in which case it represents the displayed differential; or it must also contain \mathcal{D}_1 , in which case it starts at \mathbf{Y}_0 (rather than \mathbf{Y}_2). This verifies that \mathbf{Y}_2 and \mathbf{B}_2 represents a submodule. We have seen that this submodule is acyclic. Thus, the entire module is homotopy equivalent to the quotient module (where we divide out by \mathbf{Y}_2 and \mathbf{B}_2).

We have now verified all the arrows in the quotient module of Figure 17. There are no other arrows. This can be readily seen by the following: consider the periodic domain $P = \mathcal{D}_1 + \mathcal{D}_2 + \mathcal{D}_3 - \mathcal{D}_4 + \mathcal{D}_5 + \mathcal{D}_6$. This generates the space of periodic domains locally. All possible domains connecting generators are obtained from the shown domains plus some number of copies of P . The result always has a negative local multiplicity somewhere, except in one special case: both \mathcal{D}_4 and $\mathcal{D}_1 + \mathcal{D}_2 + \mathcal{D}_3 + \mathcal{D}_5 + \mathcal{D}_6$ represent positive domains from \mathbf{A} to \mathbf{B} . But these two domains have already been considered above.

The stated homotopy equivalence follows easily. \square

7.2. The unblocked case.

Proof. We have the following further bigons:

$$\mathbf{B} \xrightarrow[\mathcal{D}_w+\mathcal{D}_z]{wz} \mathbf{A} \quad \mathbf{Y} \xrightarrow[\mathcal{D}_z]{z} \mathbf{X}$$

rectangles

$$\begin{array}{ccc} \mathbf{X}_2 & \xrightarrow[\mathcal{D}_3+\mathcal{D}_w]{w} & \mathbf{A}_2 & \quad \mathbf{A}_2 & \xrightarrow[\mathcal{D}_6+\mathcal{D}_z]{z \otimes L_2} & \mathbf{A}_1 \\ \mathbf{B}_1 & \xrightarrow[\mathcal{D}_2+\mathcal{D}_w]{w \otimes L_1} & \mathbf{Y}_0 & \quad \mathbf{X}_0 & \xrightarrow[\mathcal{D}_1+\mathcal{D}_3+\mathcal{D}_w]{w \otimes R_1} & \mathbf{A}_1 \end{array}$$

annuli:

$$\begin{array}{ccc}
\mathbf{A}_1 & \xrightarrow[\mathcal{D}_1+\mathcal{D}_2+\mathcal{D}_3+\mathcal{D}_w]{w\otimes U_1} & \mathbf{A}_1 & & {}^0\mathbf{A}_{1,2} & \xrightarrow[\mathcal{D}_1+\mathcal{D}_2+\mathcal{D}_3+\mathcal{D}_w]{w\otimes U_1} & {}^0\mathbf{A}_{1,2} \\
\mathbf{A}_2 & \xrightarrow[\mathcal{D}_5+\mathcal{D}_6+\mathcal{D}_z]{z\otimes U_2} & \mathbf{A}_2 & & {}^0\mathbf{A}_{1,2} & \xrightarrow[\mathcal{D}_5+\mathcal{D}_6+\mathcal{D}_z]{z\otimes U_2} & {}^0\mathbf{A}_{1,2} \\
\mathbf{B}_1 & \xrightarrow[\mathcal{D}_1+\mathcal{D}_2+\mathcal{D}_3+\mathcal{D}_w]{w\otimes U_1} & \mathbf{B}_1 & & {}^0\mathbf{B}_{1,2} & \xrightarrow[\mathcal{D}_1+\mathcal{D}_2+\mathcal{D}_3+\mathcal{D}_w]{w\otimes U_1} & {}^0\mathbf{B}_{1,2} \\
\mathbf{B}_2 & \xrightarrow[\mathcal{D}_5+\mathcal{D}_6+\mathcal{D}_z]{z\otimes U_2} & \mathbf{B}_2 & & {}^0\mathbf{B}_{1,2} & \xrightarrow[\mathcal{D}_5+\mathcal{D}_6+\mathcal{D}_z]{z\otimes U_2} & {}^0\mathbf{B}_{1,2} \\
\mathbf{X}_0 & \xrightarrow[\mathcal{D}_1+\mathcal{D}_2+\mathcal{D}_3+\mathcal{D}_w]{w\otimes U_1} & \mathbf{X}_0 & & {}^0\mathbf{X}_{0,2} & \xrightarrow[\mathcal{D}_1+\mathcal{D}_2+\mathcal{D}_3+\mathcal{D}_w]{w\otimes U_1} & {}^0\mathbf{X}_{0,2} \\
\mathbf{Y}_0 & \xrightarrow[\mathcal{D}_1+\mathcal{D}_2+\mathcal{D}_3+\mathcal{D}_w]{w} & \mathbf{Y}_0 & & {}^0\mathbf{Y}_{0,2} & \xrightarrow[\mathcal{D}_1+\mathcal{D}_2+\mathcal{D}_3+\mathcal{D}_w]{w} & {}^0\mathbf{Y}_{0,2}
\end{array}$$

The bigon

$$\mathbf{X} \xrightarrow[\mathcal{D}_4+\mathcal{D}_w]{w} \mathbf{Y}$$

cancels the annulus

$$\mathbf{X} \xrightarrow[\mathcal{D}_5+\mathcal{D}_6]{w} \mathbf{Y}$$

(For this last cancellation, observe that o_2 is an odd orbit according to our orbit marking; so although $\mathcal{D}_5 + \mathcal{D}_6$ does not cross the w basepoint, it does contribute w , since the corresponding rectangle contains the orbit o_2 .)

Contracting the arrow from \mathbf{Y}_2 to \mathbf{B}_2 , we obtain an action corresponding to the juxtaposition of polygons

$$\mathbf{B}_1 \xrightarrow[\mathcal{D}_5]{R_2} \mathbf{B}_2 \xleftarrow[\mathcal{D}_3]{} \mathbf{Y}_2 \xrightarrow[\mathcal{D}_z]{z} \mathbf{X}_2.$$

To summarize, we have verified the additional actions shown in Figure 19 (i.e. in addition to the ones from Figure 17).

In fact, the annuli illustrated above also demonstrate that there are no other self-arrows in the picture. For example, there is no $w \otimes U_1$ action from \mathbf{A}_2 to itself, although $\mathcal{D}_1 + \mathcal{D}_2 + \mathcal{D}_3 + \mathcal{D}_4$ gives a domain. The reason for this is that there is no corner of \mathbf{A}_2 from which we can cut in to \check{Z}_1 to get a U_1 action.

To get the stated identification

$${}^{\mathcal{B}_2^*}RQ(\mathcal{H}^{\parallel,x})_{\mathcal{B}_1^*} \boxtimes^{\mathcal{B}_1^*, \mathcal{A}_1''} \mathcal{K} \cong {}^{\mathcal{B}_2^*}V_{\mathcal{B}_1^*} \boxtimes^{\mathcal{B}_1^*, \mathcal{A}_1''} \mathcal{K},$$

we must argue that there are no further arrows in ${}^{\mathcal{B}_2^*}RQ(\mathcal{H}^{\parallel,x})_{\mathcal{B}_1^*} \boxtimes^{\mathcal{B}_1^*, \mathcal{A}_1''} \mathcal{K}$. It helps to observe that we already have no further arrows when we set $w = z = 0$; and there are no additional self-arrows.

The only other additional arrows that could be allowed by grading considerations. Consider ${}^{\mathcal{B}_2^*}RQ(\mathcal{H}^{\parallel,x})_{\mathcal{B}_1^*} \boxtimes^{\mathcal{B}_1^*, \mathcal{A}_1''} \mathcal{K}$. The relative Alexander gradings are specified by

$$\mathfrak{A}(\mathbf{A}_2) = \mathfrak{A}(\mathbf{Y}_0) = \frac{1}{2} \quad \mathfrak{A}(\mathbf{A}_1) = \mathfrak{A}(\mathbf{B}_1) = 0 \quad \mathfrak{A}(\mathbf{X}_0) = \mathfrak{A}(\mathbf{X}_2) = -\frac{1}{2},$$

and Δ -gradings by:

$$\mathbf{m}(\mathbf{A}_1) = \frac{1}{2} \quad \mathbf{m}(\mathbf{A}_2) = \mathbf{m}(\mathbf{Y}_0) = \mathbf{m}(\mathbf{X}_0) = \mathbf{m}(\mathbf{X}_2) = 0 \quad \mathbf{m}(\mathbf{B}_1) = -\frac{1}{2}.$$

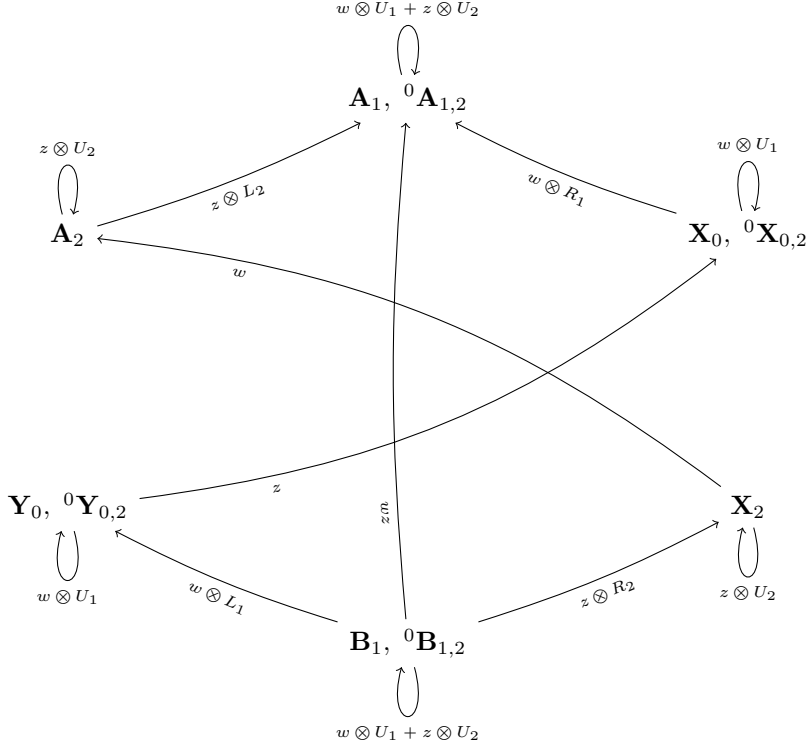


FIGURE 19. Further actions

Note also that $\mathfrak{A}(w) = -1$, $\mathfrak{m}(w) = -1$; $\mathfrak{A}(z) = 1$, $\mathfrak{m}(z) = -1$. Thus, the gradings and idempotents could allow $w\mathbf{Y}_0$ to appear in $\delta^1(\mathbf{X}_0)$ and $z\mathbf{X}_2$ to appear in $\delta^1(\mathbf{A}_2)$. (Observe here that δ^1 is taken with respect to the type DD bimodules ${}^{\mathcal{B}_2^*}RQ(\mathcal{H}^{\parallel, x})_{\mathcal{B}_1^*} \boxtimes^{\mathcal{B}_1^*, \mathcal{A}''} \mathcal{K}$; whose generators we simply identify with the generators of ${}^{\mathcal{B}_2^*}RQ(\mathcal{H}^{\parallel, x})_{\mathcal{B}_1^*}$.)

But both possibilities are excluded by $\delta^1 \circ \delta^1 = 0$.

□

8. COMPUTING LINK FLOER HOMOLOGY

Recall that if $\widehat{\mathcal{D}}$ is an upper knot diagram with associated curved algebra \mathcal{C}^* , in [9], we defined a curved type D structure ${}^{c^*}R^{alg}(\widehat{\mathcal{D}})$. This was defined by slicing up the diagram $\widehat{\mathcal{D}}$ into elementary pieces (crossings, cups, and caps), associating algebraically defined curved type DA bimodules (over \mathcal{C}) to all of those pieces, and then tensoring them together. It was then proved in [9, Theorem 16.3] that if $\widehat{\mathcal{D}}$ is an upper diagram in bridge position and \mathcal{H}^\wedge is its associated Heegaard diagram, then

$${}^{c^*}R(\mathcal{H}^\wedge) \simeq {}^{c^*}R^{alg}(\widehat{\mathcal{D}}).$$

In fact, the algebraic bimodules from [9] can all be extended to \mathcal{B}^* . Bearing this in mind, we have the following alternative characterization of ${}^{c^*}R^{alg}(\widehat{\mathcal{D}})$. Tensor the algebraic bimodules over \mathcal{B}^* to arrive at a type D structure over \mathcal{B} , which we will denote ${}^{\mathcal{B}^*}R^{alg}(\widehat{\mathcal{D}})$. Then, ${}^{c^*}R^{alg}(\widehat{\mathcal{D}})$ is the type D structure characterized by the property that

$${}^{\mathcal{B}^*}R^{alg}(\widehat{\mathcal{D}}) \simeq {}^{\mathcal{B}^*}\iota_{\mathcal{C}^*} \boxtimes {}^{c^*}R^{alg}(\widehat{\mathcal{D}}).$$

We can now extend the definition of ${}^{\mathcal{B}^*}R^{alg}(\widehat{\mathcal{D}})$ to canonically marked upper diagrams, by declaring the algebraic bimodule (over \mathcal{B}^*) associated to a marked minimum to be the bimodule defined in Section 6.

Theorem 8.1. *Let \mathcal{H}^\wedge be a canonically marked upper diagram in bridge position and \mathcal{H}^\wedge be its associated marked upper Heegaard diagram, then there is a type D structure ${}^{c^*}R^{alg}(\widehat{\mathcal{D}})$ uniquely characterized by the property that*

$${}^{\mathcal{B}^*}R^{alg}(\widehat{\mathcal{D}}) \simeq {}^{\mathcal{B}^*}\iota_{\mathcal{C}^*} \boxtimes {}^{c^*}R^{alg}(\widehat{\mathcal{D}}).$$

Moreover, there is an identification

$${}^{c^*}R(\mathcal{H}^\wedge) \simeq {}^{c^*}R^{alg}(\widehat{\mathcal{D}}).$$

The above result will be seen as a consequence of the following proposition. As in [9], a type D module ${}^{c^*}X$ is called *relevant* if there is an \mathcal{A}_∞ bimodule $Z_{\mathcal{A}''}$ with the property that

$${}^{\mathcal{B}^*}\iota_{\mathcal{C}^*} \boxtimes {}^{c^*}X \simeq Z_{\mathcal{A}''} \boxtimes^{\mathcal{A}''} {}^{\mathcal{B}^*}\mathcal{K}.$$

Proposition 8.2. *If ${}^{c_1^*}X$ is relevant, then ${}^{c_2^*}Y = {}^{c_2^*}RQ(\mathcal{H}^\parallel)_{\mathcal{C}_1^*} \boxtimes {}^{c_1^*}X$ is uniquely characterized up to homotopy by the property that*

$$(8.1) \quad {}^{\mathcal{B}_2^*}\iota_{\mathcal{C}_2^*} \boxtimes {}^{c_2^*}Y \simeq {}^{\mathcal{B}_2^*}V_{\mathcal{B}_1^*} \boxtimes {}^{\mathcal{B}_1^*}\iota_{\mathcal{C}_1^*} \boxtimes {}^{c_1^*}Y.$$

Moreover, ${}^{c_2^*}Y$ is relevant.

Proof. First, we verify Equation (8.1) (using, in order, the definition of Y , relevance of X , commutativity of \boxtimes , Proposition 7.1, and the relevance of X):

$$\begin{aligned} {}^{\mathcal{B}_2^*}\iota_{\mathcal{C}_2^*} \boxtimes {}^{c^*}Y &= {}^{\mathcal{B}_2^*}\iota_{\mathcal{C}_2^*} \boxtimes {}^{c_2^*}RQ(\mathcal{H}^\parallel)_{\mathcal{C}_1^*} \boxtimes {}^{c_1^*}X \\ &\simeq {}^{\mathcal{B}_2^*}RQ^x(\mathcal{H}^{\parallel,x})_{\mathcal{B}_1^*} \boxtimes {}^{\mathcal{B}_2^*}\iota_{\mathcal{C}_2^*} \boxtimes {}^{c_1^*}X \\ &\simeq {}^{\mathcal{B}_2^*}RQ^x(\mathcal{H}^{\parallel,x})_{\mathcal{B}_1^*} \boxtimes (Z_{\mathcal{A}_1''} \boxtimes {}^{\mathcal{B}_1^*}\mathcal{K}) \\ &\simeq Z_{\mathcal{A}_1''} \boxtimes ({}^{\mathcal{B}_2^*}RQ^x(\mathcal{H}^{\parallel,x})_{\mathcal{B}_1^*} \boxtimes {}^{\mathcal{B}_1^*}\mathcal{K}) \\ &\simeq Z_{\mathcal{A}_1''} \boxtimes ({}^{\mathcal{B}_2^*}V_{\mathcal{B}_1^*} \boxtimes {}^{\mathcal{B}_1^*}\mathcal{K}) \\ &\simeq {}^{\mathcal{B}_2^*}V_{\mathcal{B}_1^*} \boxtimes (Z_{\mathcal{A}_1''} \boxtimes {}^{\mathcal{B}_1^*}\mathcal{K}) \\ &\simeq {}^{\mathcal{B}_2^*}V_{\mathcal{B}_1^*} \boxtimes {}^{\mathcal{B}_2^*}\iota_{\mathcal{C}_2^*} \boxtimes {}^{c_1^*}X. \end{aligned}$$

Equation (8.1) uniquely characterizes ${}^{c_2^*}Y$, according to Lemma 4.3.

To see C^*Y is relevant, we use the above computation and Proposition 6.5, as follows:

$$\begin{aligned} \mathcal{B}_2^* \iota_{C_2^*} \boxtimes C^*Y &\simeq Z_{\mathcal{A}_1''} \boxtimes (\mathcal{B}_2^* V_{\mathcal{B}_1^*} \boxtimes \mathcal{B}_1^*, \mathcal{A}_1'' \mathcal{K}) \\ &\simeq Z_{\mathcal{A}_1''} \boxtimes (\mathcal{A}_1'' V'_{\mathcal{A}_2''} \boxtimes \mathcal{A}_2'', \mathcal{B}_2^* \mathcal{K}) = (Z_{\mathcal{A}_1''} \boxtimes \mathcal{A}_1'' V'_{\mathcal{A}_2''}) \boxtimes \mathcal{A}_2'', \mathcal{B}_2^* \mathcal{K} \end{aligned}$$

□

Proof of Theorem 8.1. We prove by induction on the number of components that $C^*R^{alg}(\widehat{\mathcal{D}})$ is relevant. The case of one component was proved in [9]. The inductive hypothesis then follows from Proposition 8.2. □

Let \mathcal{D} be a canonically marked planar diagram for an oriented link, and let $\widehat{\mathcal{D}}$ be the upper diagram obtained by removing the global minimum, and \mathcal{H}^\wedge be its associated upper diagram. The output algebra $\mathcal{C}(1)$ of $\widehat{\mathcal{D}}$ is identified with

$$\mathbb{F}[U_1, U_2]/U_1 U_2.$$

There is a ring isomorphism

$$\Psi: \mathcal{C}(1) \rightarrow \mathbb{F}[w_1, z_1]/w_1 z_1,$$

sending U_1 to w_1 and U_2 to z_1 .

Theorem 8.3. *For any Heegaard diagram \mathcal{H} representing \vec{L}^+ , there is a chain homotopy equivalence*

$$CFL(\mathcal{H}) \simeq [\Psi]_{\mathcal{C}(1)} \boxtimes R^{alg}(\widehat{\mathcal{D}}).$$

Proof. The bimodule $\mathbb{F}[w, z]/wz[\Psi]_{\mathcal{C}(1)}$ can be thought of as the type A module associated to the global minimum. (See [9, Lemma 8.14]. Thus, the lemma can be seen as a consequence of (a particular easy special case of) the pairing theorem. □

Proof of Theorem 1.2. This follows from Theorem 8.3, by specializing to

$$w_1 = z_1 = \cdots = w_\ell = z_\ell = 0.$$

□

8.1. Restricting idempotents. In our computations, we do not need the full bimodule $\mathcal{B}_2^* V_{\mathcal{B}_1^*}$, as we are able to work over C^* . Thus, for computations, it suffices to use only $\mathcal{B}_2^* V_{\mathcal{B}_1^*} \boxtimes \mathcal{B}_1^* \iota_{C_1^*}$. The actions for this bimodule are described in Figure 20; see also Figure 21 for $\mathcal{B}_2^* \widehat{V}_{\mathcal{B}_1^*} \boxtimes \mathcal{B}_1^* \iota_{C_1^*}$.

$$\mathcal{B}^{(n, M')} V_{\mathcal{C}(n+1, M)} = \mathcal{B}^{(n, M')} V_{\mathcal{B}(n+1, M)} \boxtimes^{\mathcal{B}(n+1)} i_{\mathcal{C}(n+1)} :$$

REFERENCES

- [1] L. H. Kauffman. *Formal knot theory*. Number 30 in Mathematical Notes. Princeton University Press, 1983.
- [2] R. Lipshitz. A cylindrical reformulation of Heegaard Floer homology. *Geom. Topol.*, 10:955–1097 (electronic), 2006.
- [3] R. Lipshitz, P. S. Ozsváth, and D. P. Thurston. Bimodules in bordered Heegaard Floer homology. *Geom. Topol.*, 19(2):525–724, 2015.
- [4] R. Lipshitz, P. S. Ozsváth, and D. P. Thurston. Bordered Heegaard Floer homology. *Mem. Amer. Math. Soc.*, 254(1216):viii+279, 2018.

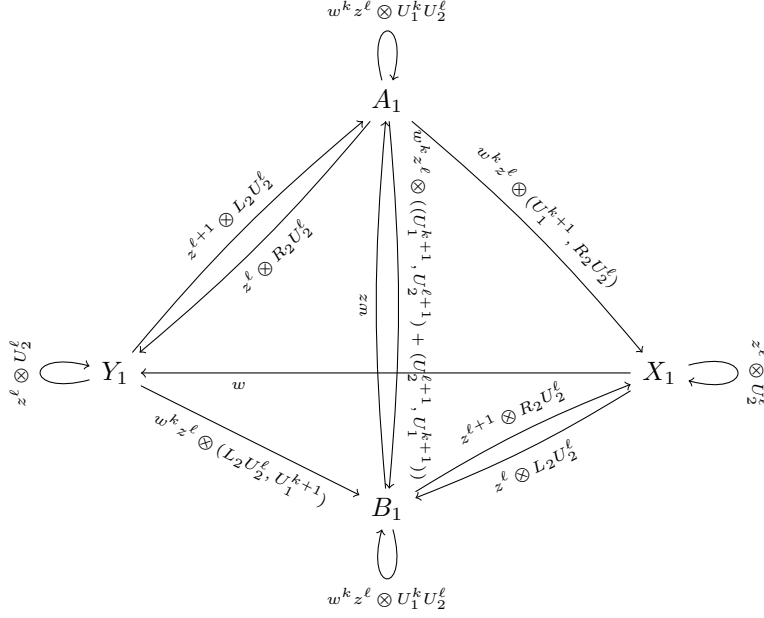


FIGURE 20. Actions for $\mathcal{B}_2^* V_{\mathcal{B}_1^*} \boxtimes^{\mathcal{B}_1^*} \mathcal{L}_{\mathcal{C}_1^*}$

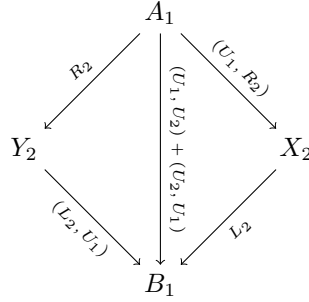


FIGURE 21. Actions for $\mathcal{B}_2^* \widehat{V}_{\mathcal{B}_1^*} \boxtimes^{\mathcal{B}_1^*} \mathcal{L}_{\mathcal{C}_1^*}$

[5] C. Manolescu, P. S. Ozsváth, and S. Sarkar. A combinatorial description of knot Floer homology. *Ann. of Math. (2)*, 169(2):633–660, 2009.

[6] C. Manolescu, P. S. Ozsváth, Z. Szabó, and D. P. Thurston. On combinatorial link Floer homology. *Geom. Topol.*, 11:2339–2412, 2007.

[7] Y. Ni. A note on knot Floer homology of links. *Geom. Topol.*, 10:695–713, 2006.

[8] P. S. Ozsváth, A. I. Stipsicz, and Z. Szabó. *Grid homology for knots and links*, volume 208 of *Mathematical Surveys and Monographs*. American Mathematical Society, Providence, RI, 2015.

[9] P. S. Ozsváth and Z. Szabó. Algebras with matchings and knot Floer homology. In preparation.

[10] P. S. Ozsváth and Z. Szabó. Kauffman states, bordered algebras, and a bigraded knot invariant.

[11] P. S. Ozsváth and Z. Szabó. Heegaard Floer homology and alternating knots. *Geom. Topol.*, 7:225–254 (electronic), 2003.

- [12] P. S. Ozsváth and Z. Szabó. Heegaard Floer homology and alternating knots. *Geom. Topol.*, 7:225–254, 2003.
- [13] P. S. Ozsváth and Z. Szabó. Holomorphic disks and topological invariants for closed three-manifolds. *Ann. of Math. (2)*, 159(3):1027–1158, 2004.
- [14] P. S. Ozsváth and Z. Szabó. Holomorphic disks, link invariants and the multi-variable Alexander polynomial. *Algebr. Geom. Topol.*, 8(2):615–692, 2008.
- [15] P. S. Ozsváth and Z. Szabó. Link Floer homology and the Thurston norm. *J. Amer. Math. Soc.*, 21(3):671–709, 2008.

DEPARTMENT OF MATHEMATICS, PRINCETON UNIVERSITY, PRINCETON, NEW JERSEY 08544

E-mail address: `petero@math.princeton.edu`

DEPARTMENT OF MATHEMATICS, PRINCETON UNIVERSITY, PRINCETON, NEW JERSEY 08544

E-mail address: `szabo@math.princeton.edu`